

**Aircraft Measurements of Turbulence in the Stably
Stratified Atmosphere: Analysis of Cliff-Ramp
Patterns, Refractive Turbulence and Waves in the
Troposphere and Boundary Layer**

Report 3

Prepared by:

Donald Wroblewski, DEW Consulting

Prepared for:

Jorg Hacker, Airborne Research Australia

Owen Cote: Air Force Research Laboratory

Report Documentation Page

Form Approved
OMB No. 0704-0188

Public reporting burden for the collection of information is estimated to average 1 hour per response, including the time for reviewing instructions, searching existing data sources, gathering and maintaining the data needed, and completing and reviewing the collection of information. Send comments regarding this burden estimate or any other aspect of this collection of information, including suggestions for reducing this burden, to Washington Headquarters Services, Directorate for Information Operations and Reports, 1215 Jefferson Davis Highway, Suite 1204, Arlington VA 22202-4302. Respondents should be aware that notwithstanding any other provision of law, no person shall be subject to a penalty for failing to comply with a collection of information if it does not display a currently valid OMB control number.

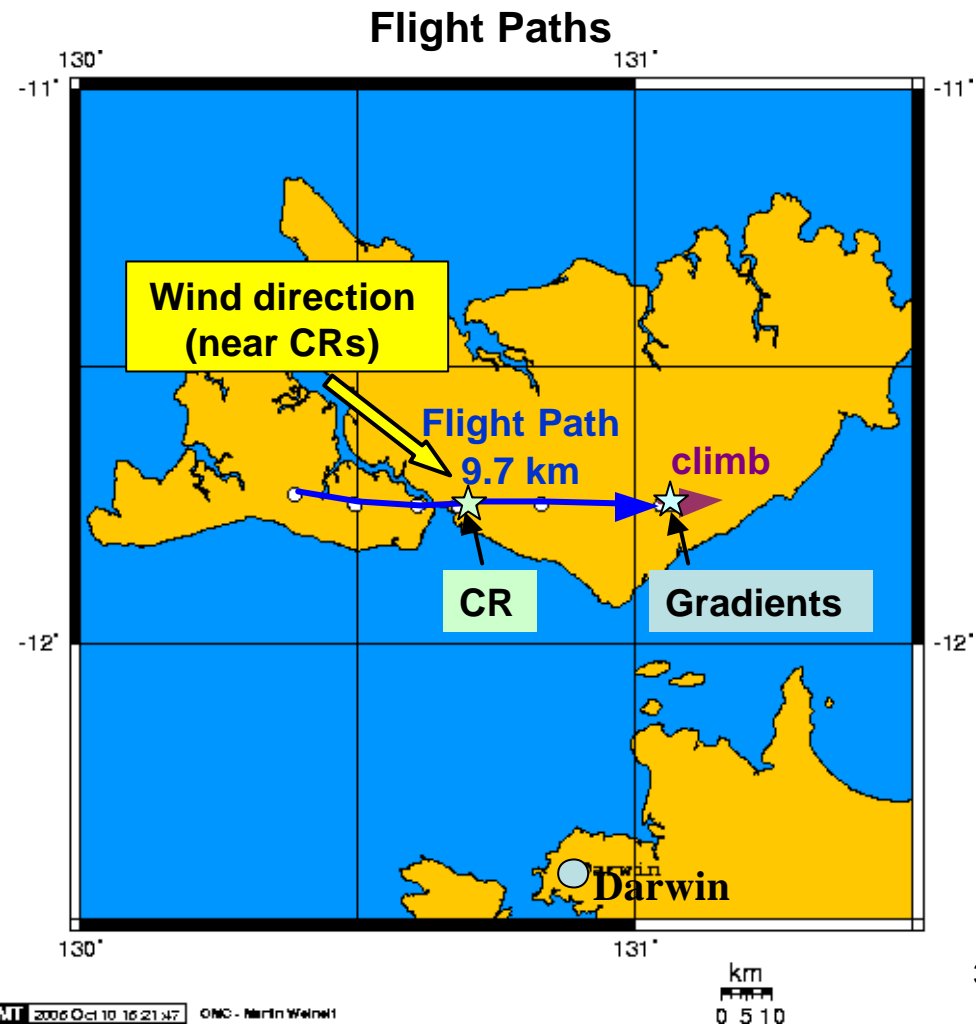
1. REPORT DATE 27 JUL 2006		2. REPORT TYPE Final Report (Technical)		3. DATES COVERED 10-05-2005 to 01-03-2006	
4. TITLE AND SUBTITLE Atmospheric Turbulence Data				5a. CONTRACT NUMBER FA520905P0445	
				5b. GRANT NUMBER	
				5c. PROGRAM ELEMENT NUMBER	
6. AUTHOR(S) Hacker Jorg				5d. PROJECT NUMBER	
				5e. TASK NUMBER	
				5f. WORK UNIT NUMBER	
7. PERFORMING ORGANIZATION NAME(S) AND ADDRESS(ES) ARA-Airborne Research Australia Pty Ltd, PO Box 335, Salisbury South 5106, Australia, AU, 5106				8. PERFORMING ORGANIZATION REPORT NUMBER AOARD-054080	
9. SPONSORING/MONITORING AGENCY NAME(S) AND ADDRESS(ES) The US Resarch Labolatory, AOARD/AFOSR, Unit 45002, APO, AP, 96337-5002				10. SPONSOR/MONITOR'S ACRONYM(S) AOARD/AFOSR	
				11. SPONSOR/MONITOR'S REPORT NUMBER(S) AOARD-054080	
12. DISTRIBUTION/AVAILABILITY STATEMENT Approved for public release; distribution unlimited					
13. SUPPLEMENTARY NOTES					
14. ABSTRACT This slide presentation is the final report of a project to measure turbulence in several high altitude formations over Southern Australia. Aircraft Measurements of Turbulence in the Stably Stratified Atmosphere: Analysis of Cliff-Ramp Patterns, Refractive Turbulence and Waves in the Troposphere and Boundary Layer					
15. SUBJECT TERMS Turbulence Modeling, clear air turbulence, optical turbulence					
16. SECURITY CLASSIFICATION OF:			17. LIMITATION OF ABSTRACT	18. NUMBER OF PAGES 44	19a. NAME OF RESPONSIBLE PERSON
a. REPORT unclassified	b. ABSTRACT unclassified	c. THIS PAGE unclassified			

OUTLINE/TABLE OF CONTENTS

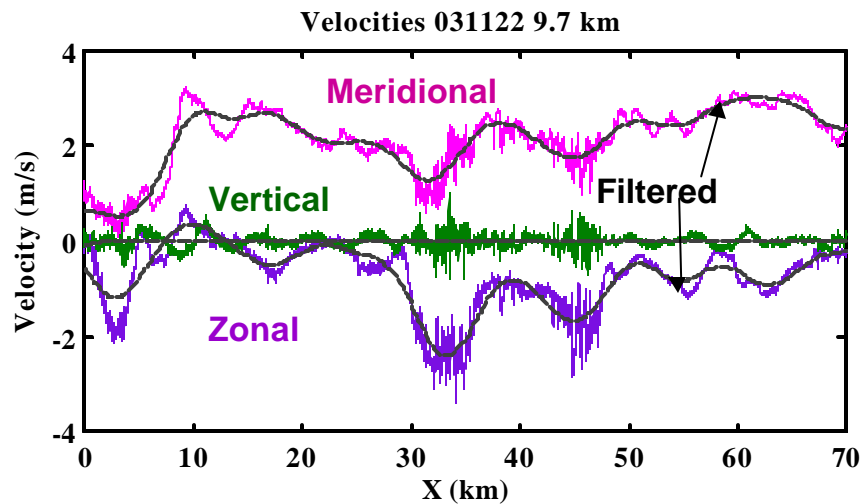
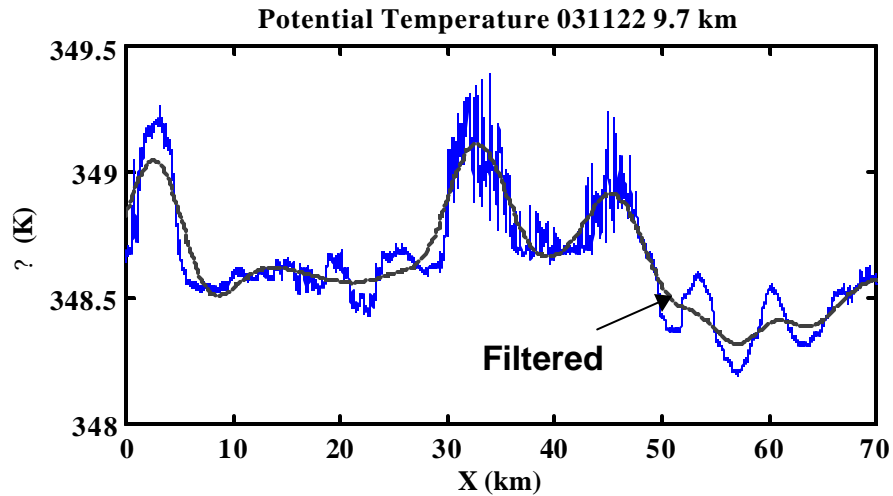
- **Cliff-Ramp Structures: 031122 (EMERALD 2):**
 - Flight paths, orientation and general conditions [slides 3-9](#)
 - High pass filtered signals [slides 10-12](#)
 - Band pass filtered signals and correlations [slides 13-16](#)
 - Structure function and billow height estimate [slide 17-18](#)
- **Cliff-Ramp Structures: 040922 during climb segment:**
 - Flight paths, orientation and general conditions [slides 19-24](#)
 - High pass filtered signals [slides 25-27](#)
 - Band pass filtered signals and correlations [slides 28-31](#)
 - Structure function and billow height estimate [slide 32-34](#)
- **Comparison of 031122 and 040922 with DNS and other CR cases**
 - Aspect ratio Wave features [slides 35-36](#)
 - Turbulence scaling [slides 37-38](#)
 - Length scale and layer “age” [slides 39-42](#)
 - Scaling with turbulent Reynolds numbers [slide 43](#)
- **Summary [slide 44](#)**

CLIFF RAMPS: 9.7 km SEGMENT ON 031122 (EMERALD 2)

- Segment is across and below outflow of thunderstorm.
- CR's seen near middle of segment
- Vertical gradients estimated during climb out at end of segment

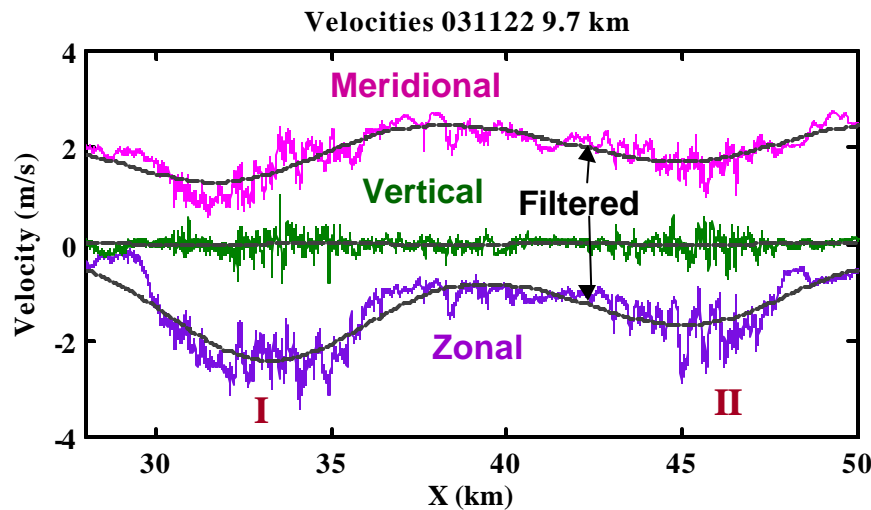
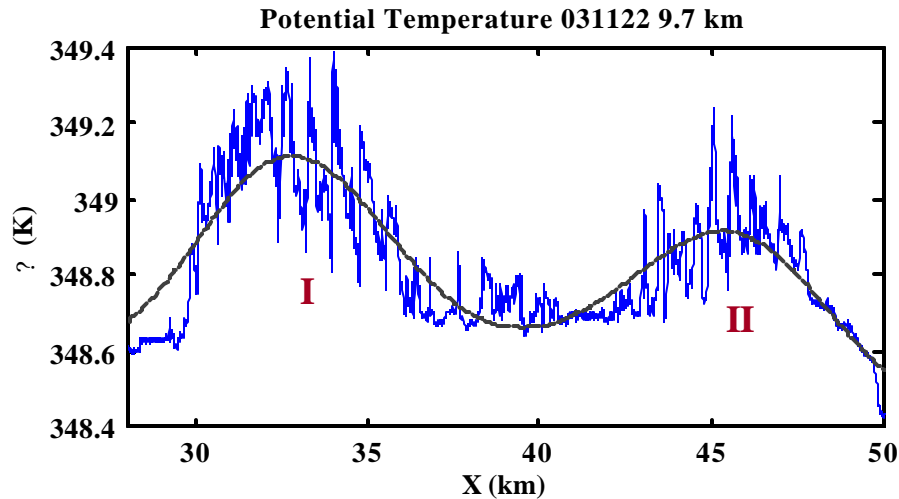


RAW PROFILES



- Low pass filtered data (dashed lines)
 - 4th order Butterworth filter, with 8.25 km cutoff wavelength
 - Use to de-trend signals to better analyze CR behavior (free of low frequency variations).
- Filtered data reveal wavelike pattern in temperature and in zonal and meridional velocities, especially around cliff ramps (30-40 km)
 - Wave features also present in vertical velocity, but these are not seen in plot due to vertical scale.

RAW PROFILES: CLOSEUP ON CLIFF RAMP REGION



- Close-up better highlights both CR structures in temperature and wavelike features in temperature and velocity.

- Wave has wavelength of about 12 km.

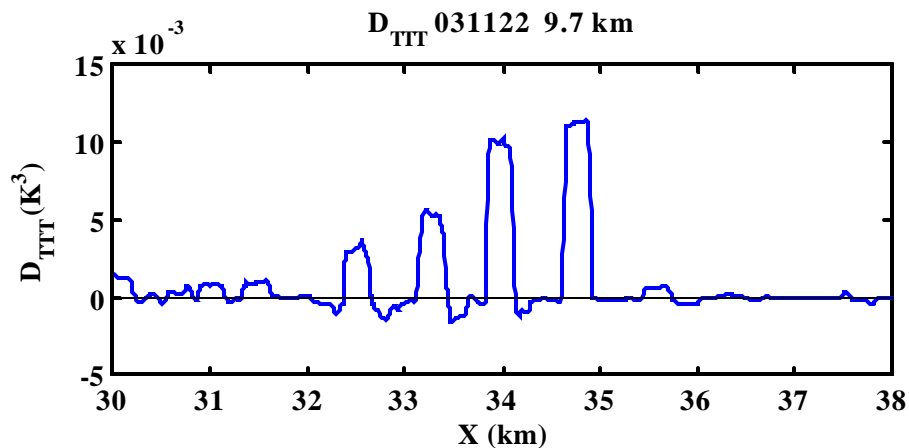
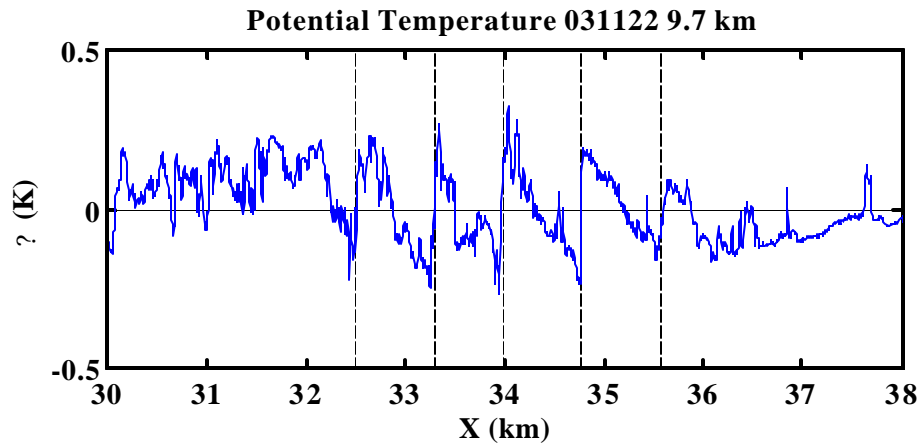
- Temperature and velocities appear to be 180 degrees out of phase.

- CRs appear near peak in temperature wave.

- Wind speeds are small– less than 3.5 m/s.

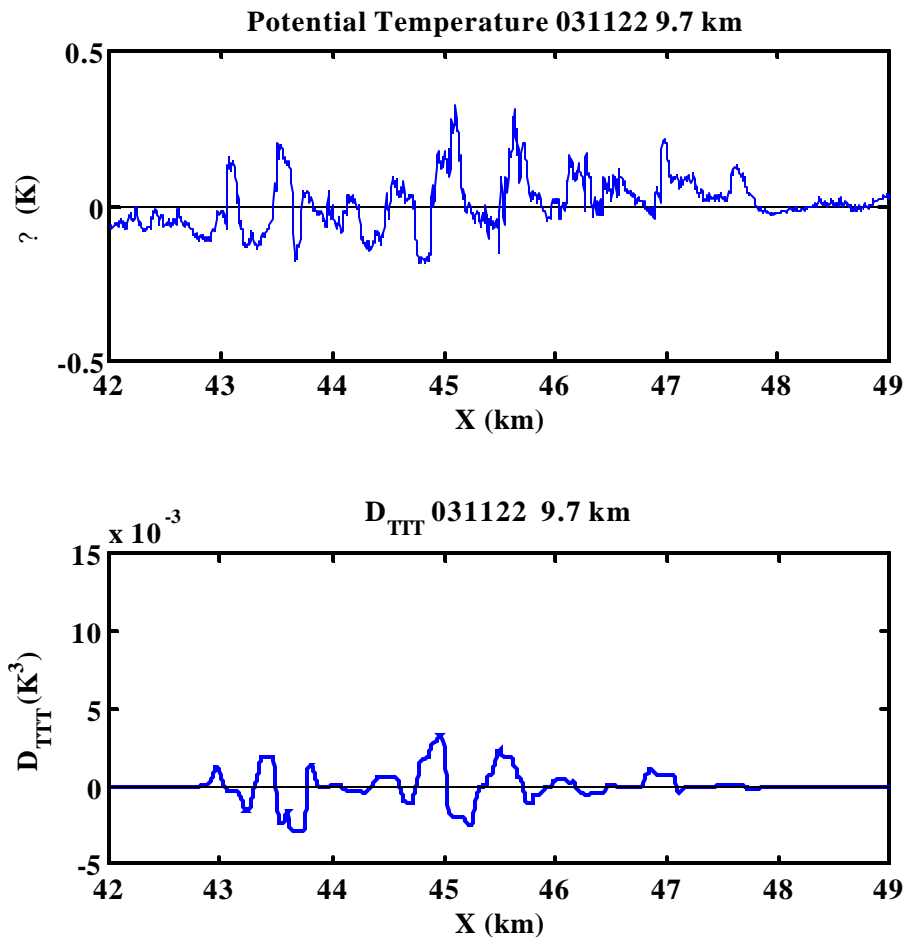
- Explore two zones with possible CRs **I** and **II**

HIGH PASS FILTERED POTENTIAL TEMPERATURE: I



- 5 distinct cliffs, though last one looks weaker than others
- Pattern is very regular
- Are these CRs or RCs?
 - First cliff seems to be preceded by ramp, but last cliff is also followed by a ramp.
- Third order structure function confirms cliffs
 - Also confirms cliff 5 is weaker than others.

HIGH PASS FILTERED POTENTIAL TEMPERATURE II

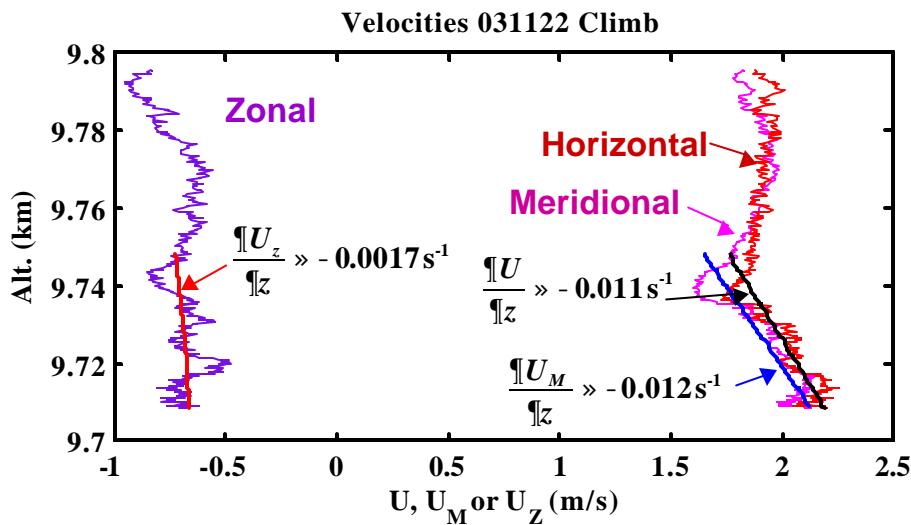
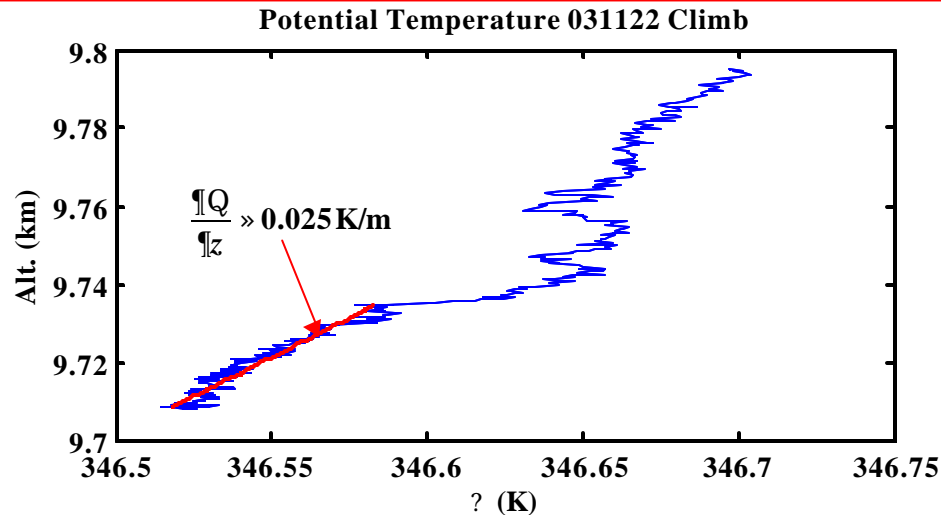


- Closeup of Zone II does not reveal distinct CR patterns, though some structures are evident with approximately the same wavelength as the CRs in Zone I.

- Third order structure function confirms that structures are weaker than cliffs in Zone I (same y axis scale as previous slide) and reveals that they are symmetric.

- Are these KH either before or after cliffs form (degraded cliffs?)

CLIMBOUT DATA AND GRADIENT ESTIMATES



- Gradients found by fitting data at beginning of climb-out from 9.7 km.

- Meridional, zonal and horizontal (in mean wind direction) velocities all display negative vertical gradients

- Relatively strong gradients considering the weak winds.

- Some uncertainty associated with choosing appropriate range for curve fit.

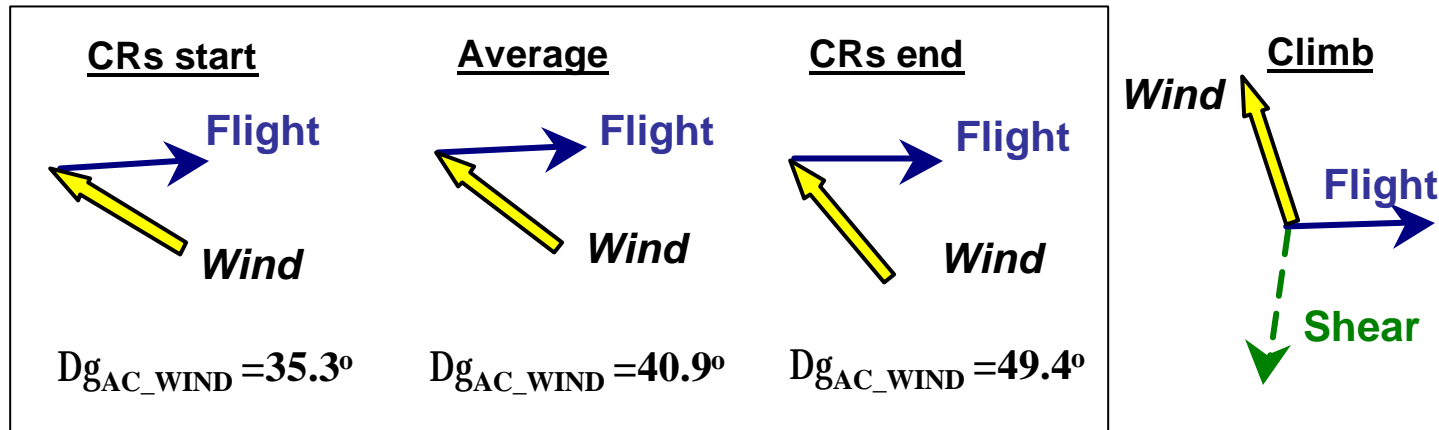
- Ri number estimate

- $S_z = 0.0123 \text{ s}^{-1}$

- $N_z = 0.0084 \text{ s}^{-1}$

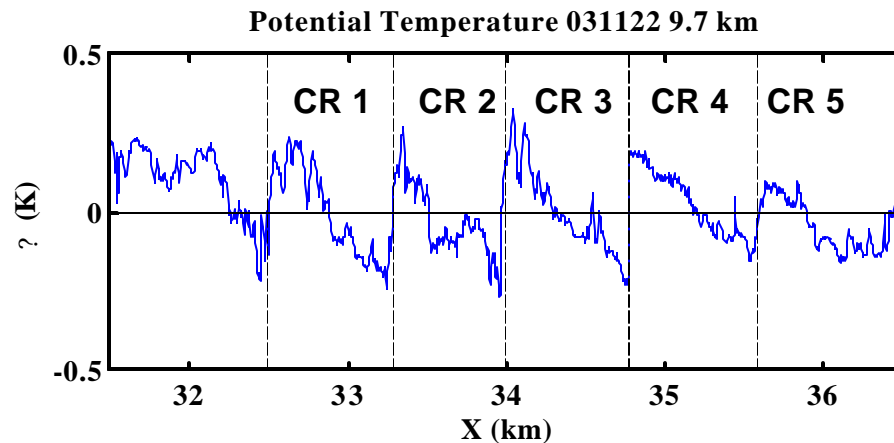
- $Ri = 0.47$

DIRECTIONS AND FLIGHT PATHS



- In proximity to CRs (boxed sketches)
 - Along-wind component of flight path is against wind
 - 35 to 50 degree difference between wind flight directions.
- During climb-out from 9.7 km
 - Flight and wind directions are nearly perpendicular
 - Shear and wind directions are almost along same line
 - Opposite directions consistent with negative shear
- Large difference between wind directions near CRs and during climb raises doubts about relevance of the gradients estimated during climb to the behavior of CRs

CR DIMENSIONS



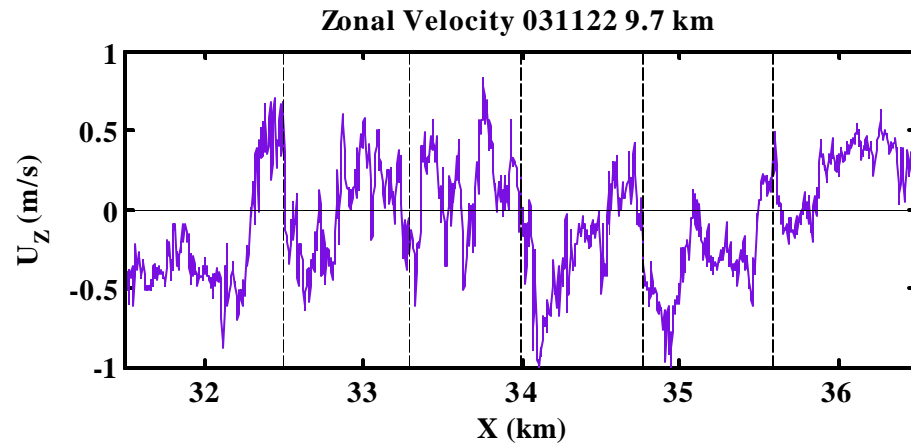
- Wavelengths: in flight direction (and wind direction)

- CR 1: 800 m (642 m)
- CR 2: 708 m (548 m)
- CR 3: 806 m (604 m)
- CR 4: 777 m (544 m)
- CR 5: 600 m (375 m)

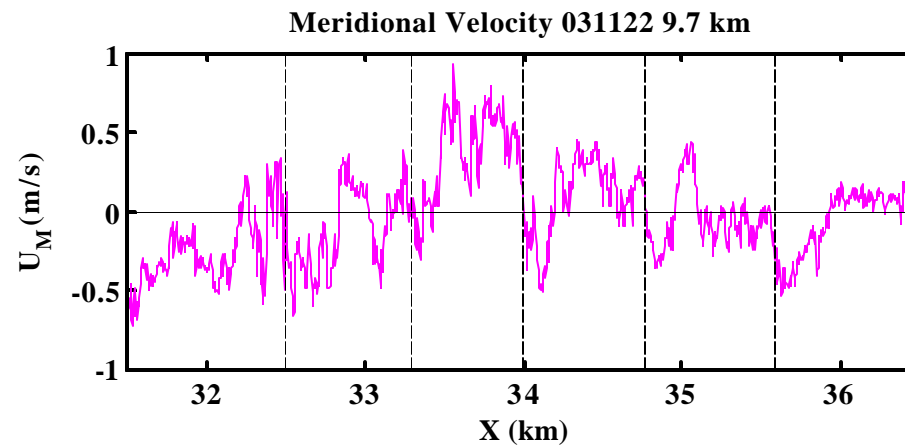
- Why do we see CRs if shear is negative?

- Would expect to see RC like 000606.

HIGH PASS FILTERED POTENTIAL TEMPERATURE

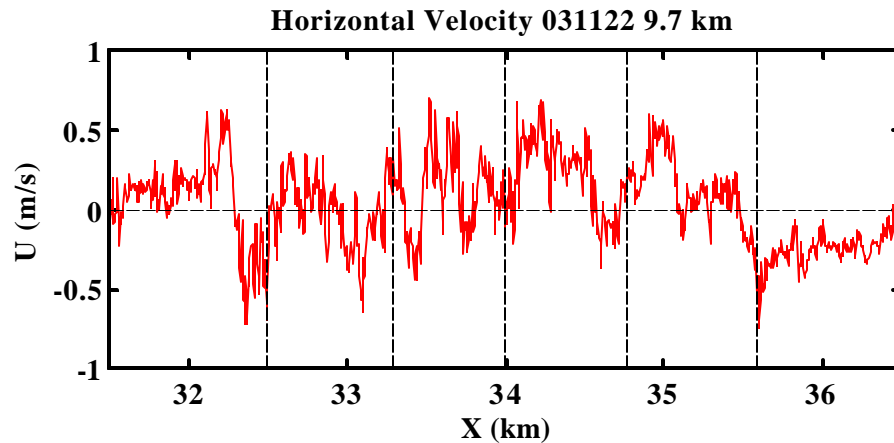


- Zonal velocity decrease coincident with temperature cliffs
- Consistent with negative vertical shear



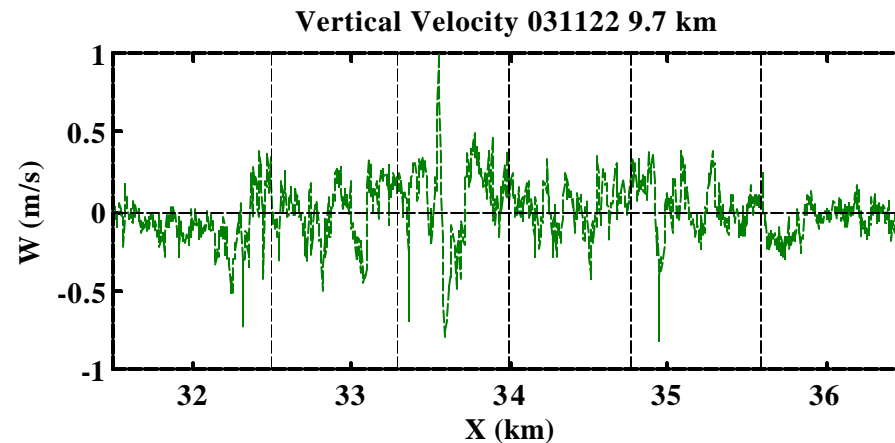
- Meridional velocity decrease coincident with temperature cliffs
- Also consistent with negative vertical shear

HIGH PASS FILTERED POTENTIAL TEMPERATURE



- Horizontal velocity sometimes increases at cliff and sometimes decreases.

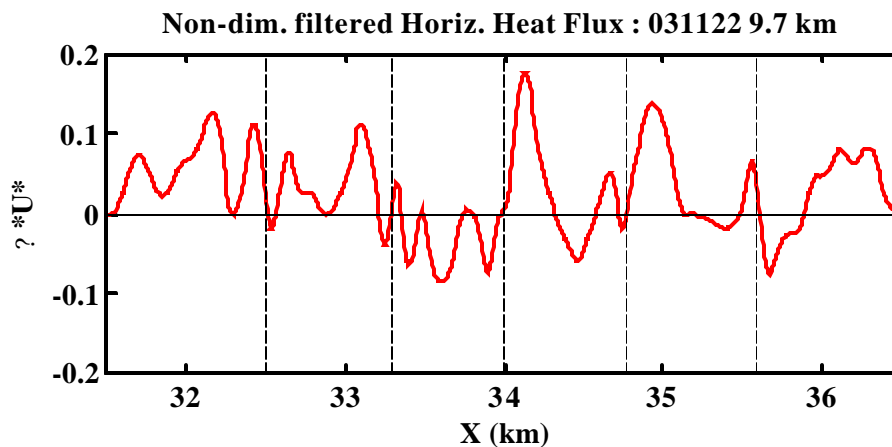
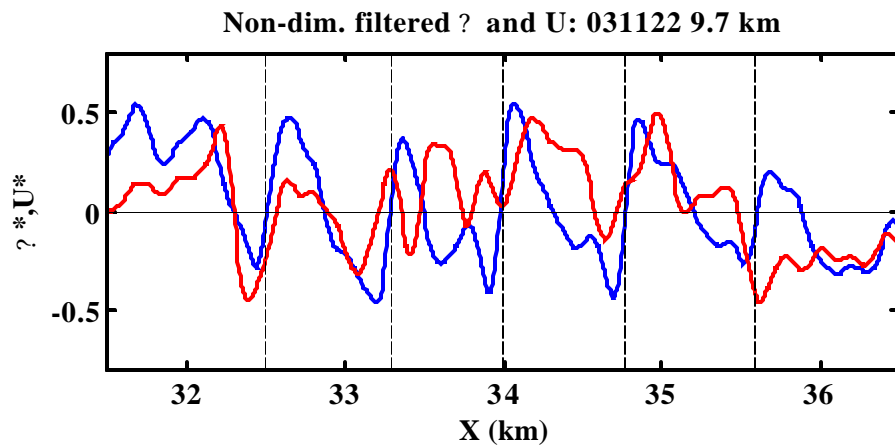
- Would expect decrease if shear is negative



- Vertical velocity fluctuations increase near cliffs

- Some large scale pattern seen, though correlation with temperature unclear.

BAND-PASS FILTERED TEMP. AND HORIZ. VELOCITY



- Overall positive correlation evident, but inconsistent during cliffs.

- Positive correlation for cliffs 1, 3 and 4, negative for 5, uncertain for 2.

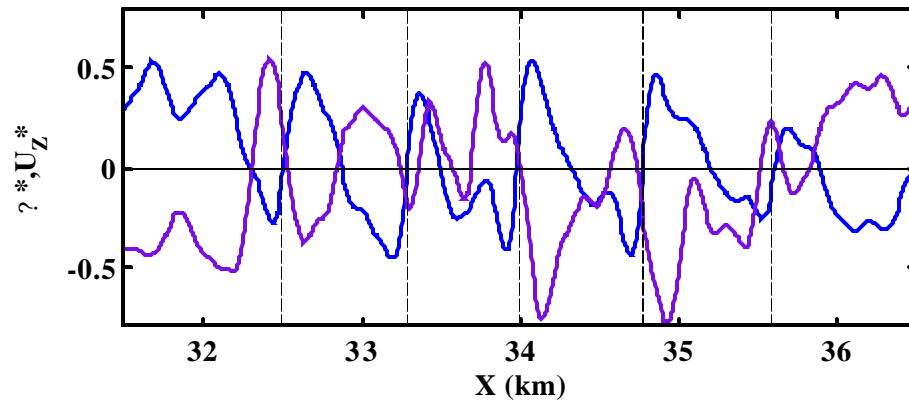
- Correlation coefficient relatively low compared to CRs from other flights

$$C_{Q^*U^*} = 0.43$$

- Heat flux echoes lack of consistent correlation

BAND-PASS FILTERED TEMP. AND ZONAL VELOCITY

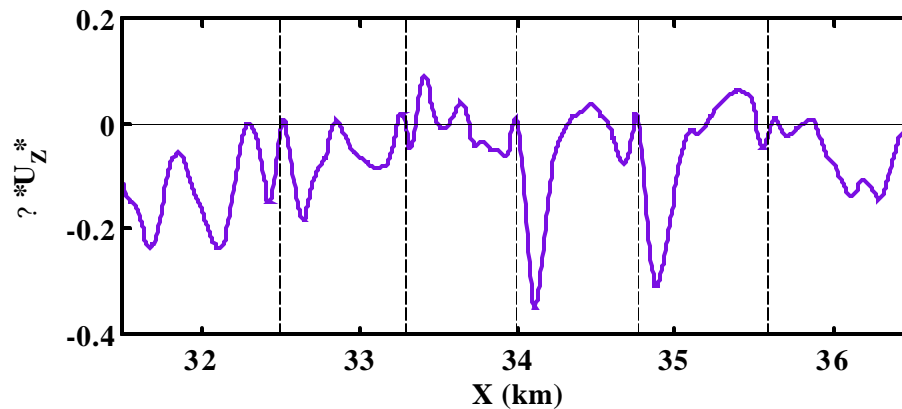
Non-dim. filtered θ and U_z : 031122 9.7 km



- Mostly negative correlation.
- Higher correlation coefficient than for horizontal velocity.

$$C_{\theta^*U_z^*} = -0.73$$

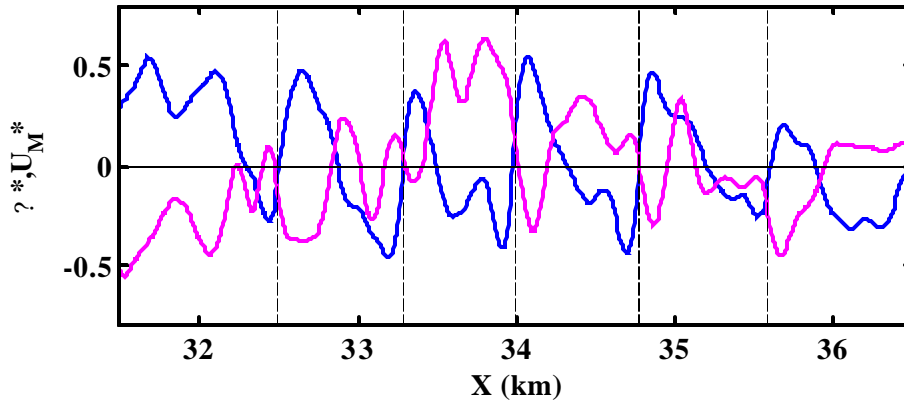
Non-dim. filtered Horiz. Heat Flux : 031122 9.7 km



- Heat flux almost entirely negative, with two bursts near cliffs 3 and 4.

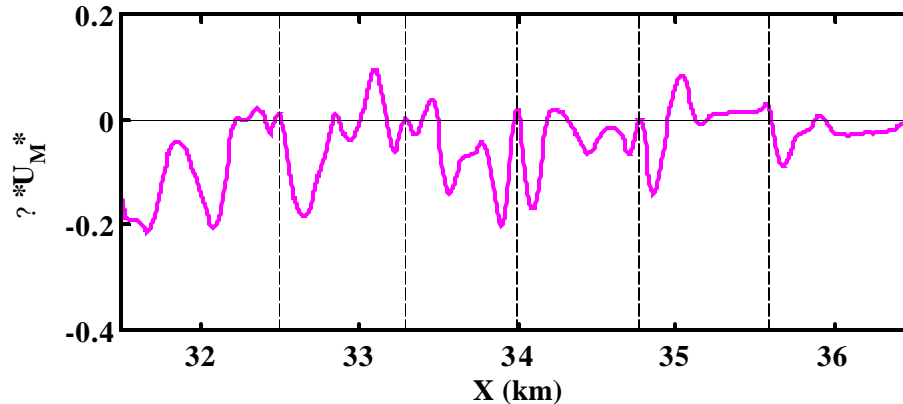
BAND-PASS FILTERED TEMP. AND MERID. VELOCITY

Non-dim. filtered θ and U_M : 031122 9.7 km



- Mostly negative correlation.
- Higher correlation coefficient than for horizontal velocity, though smaller than zonal velocity.

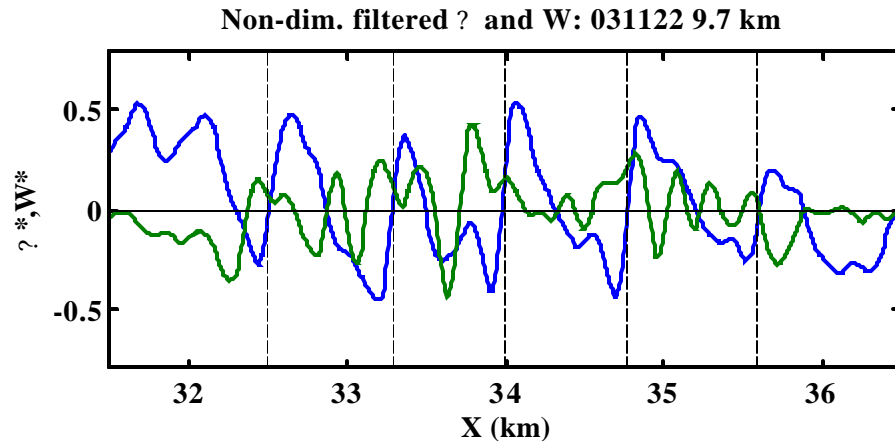
Non-dim. filtered Horiz. Heat Flux : 031122 9.7 km



$$C_{\theta^*U_M^*} = -0.62$$

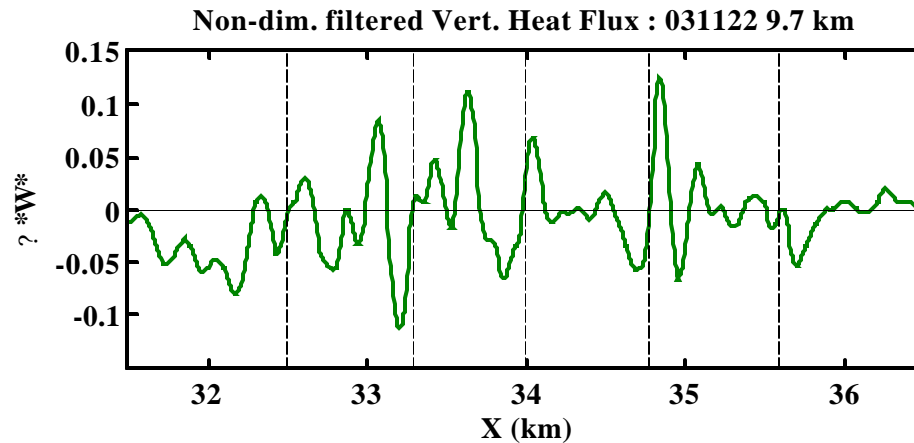
- Heat flux almost entirely negative– don't see two bursts near cliffs 3 and 4 that were seen in zonal heat flux.

BAND-PASS FILTERED TEMP. AND VERTICAL VELOCITY



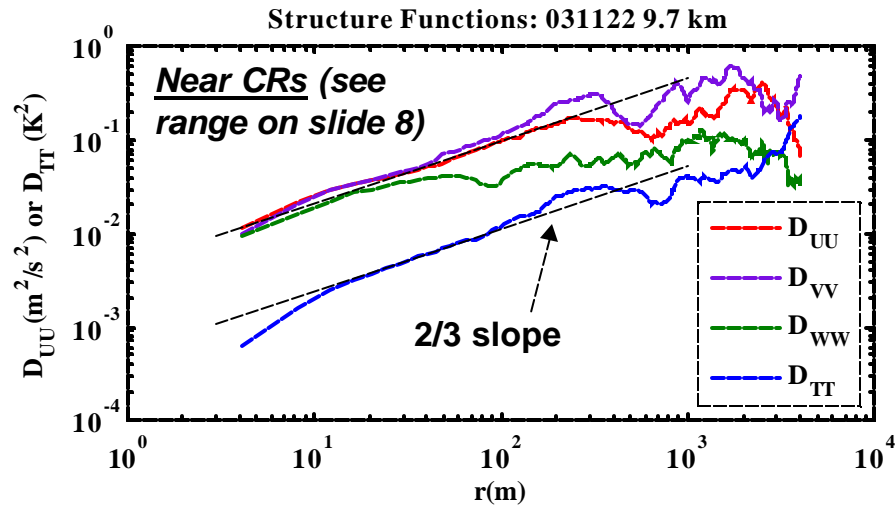
- W seems to be 180 degree out of phase with q near cliffs, with decreasing W during cliffs (4th cliff is exception)
- Correlation coefficient about the same as for CRs seen in other flights

$$C_{Q^*W^*} = -0.22$$



- Vertical heat flux shows both negative and positive bursts near cliffs.

STRUCTURE FUNCTIONS & CONSTANTS



- Near CRs (top plot)

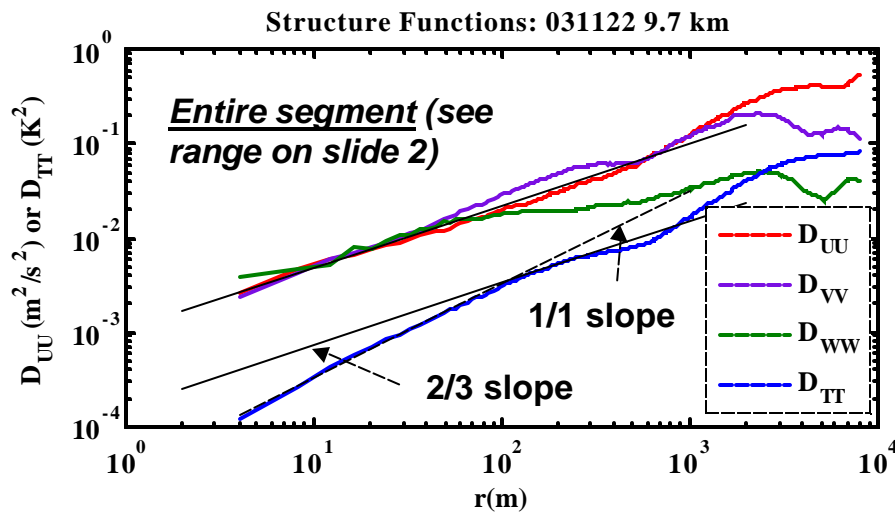
$$C_T^2 = 0.000511$$

$$C_U^2 = 0.00445 = 8.7 C_T^2$$

$$C_V^2 = 0.00501 = 1.14 C_U^2$$

$$C_W^2 = 0.00393 = 0.88 C_U^2$$

- For entire 9.7 km segment (bottom plot)



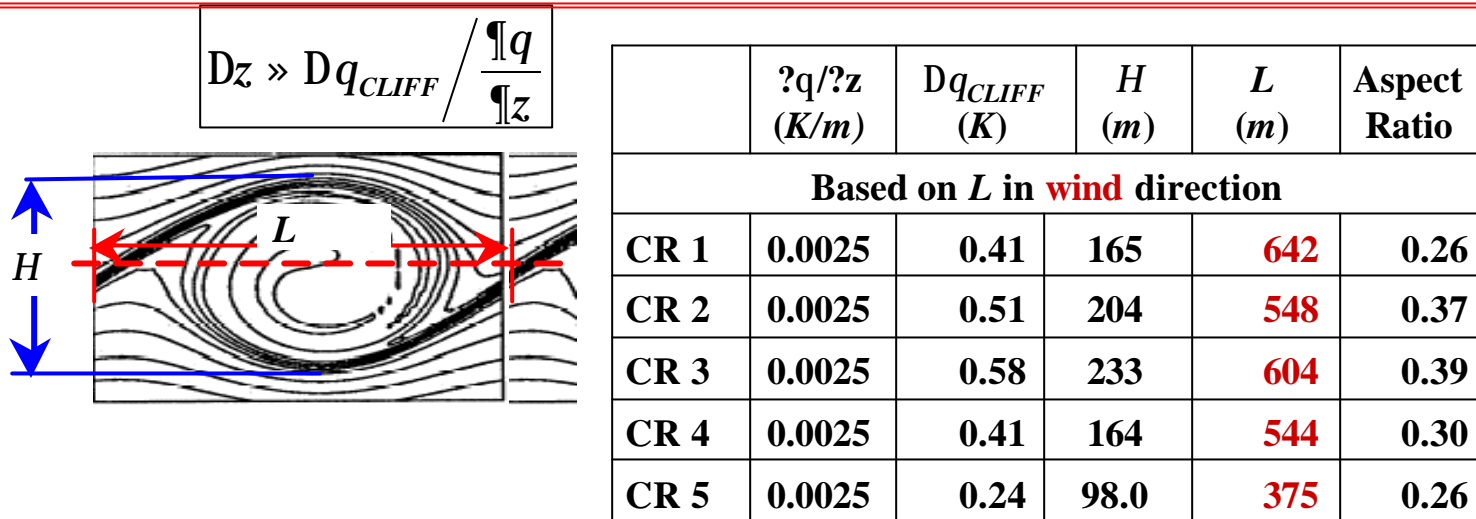
$$C_T^2 = 0.000151$$

$$C_U^2 = 0.0011 = 6.8 C_T^2$$

$$C_V^2 \approx C_W^2 \approx C_U^2$$

- Values lower than those near CRs
- D_{TT} exhibits slope of 1 below 100 m (dashed line)

BILLOW HEIGHT AND ASPECT RATIO: 031122

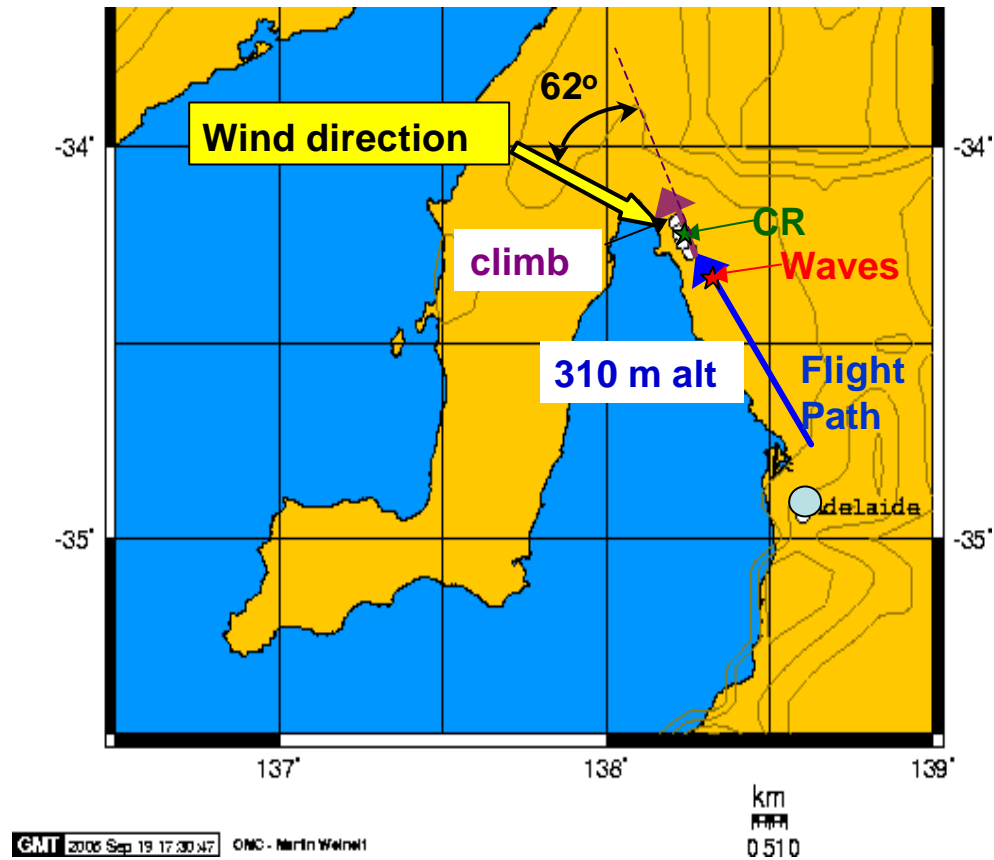


- Billow height ranges from 98 to 233 meters, resulting in aspect ratios of 0.26 to 0.39.
 - Last cliff is weak– exclude from averages
 - Average height = 191 m
 - Aspect ratios are similar to those found for CRs for other flights. See slide.

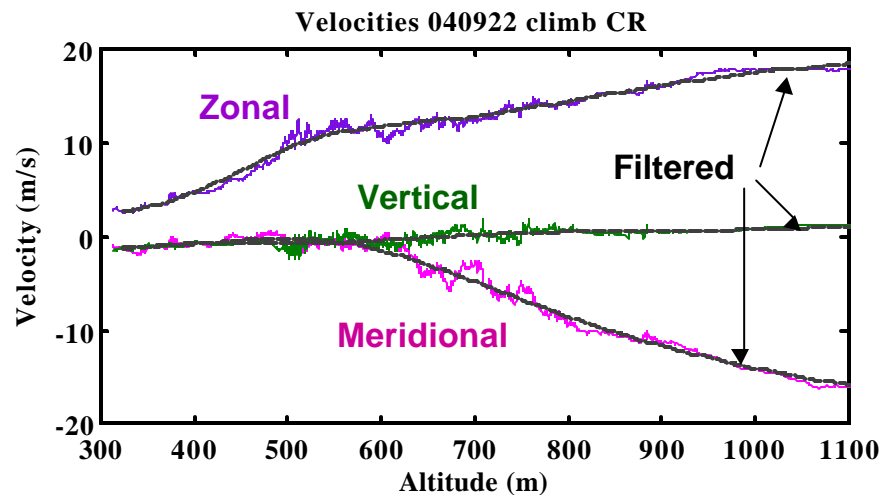
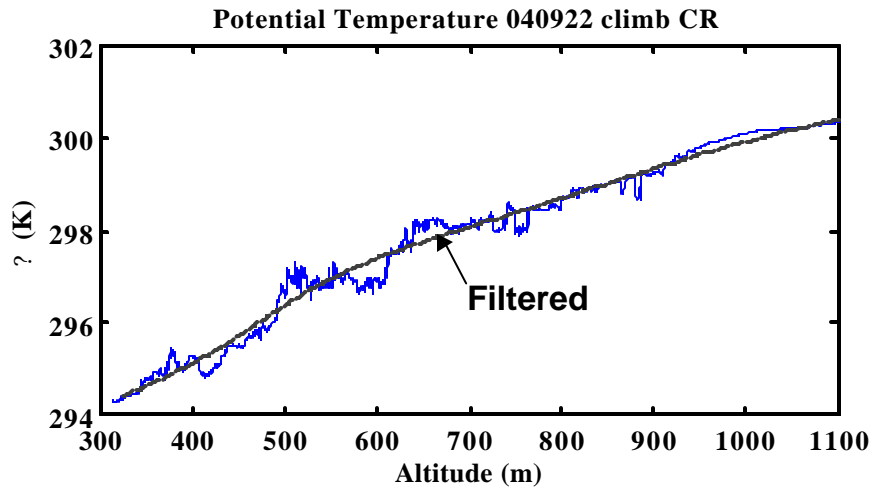
CLIFF RAMPS: CLIMB IN BOUNDARY LAYER ON 040922

- 310 m level featured very distinct waves (see Briefing 2)
- Cliff ramps seen during climb out segment following 310 m segment.

Flight Paths

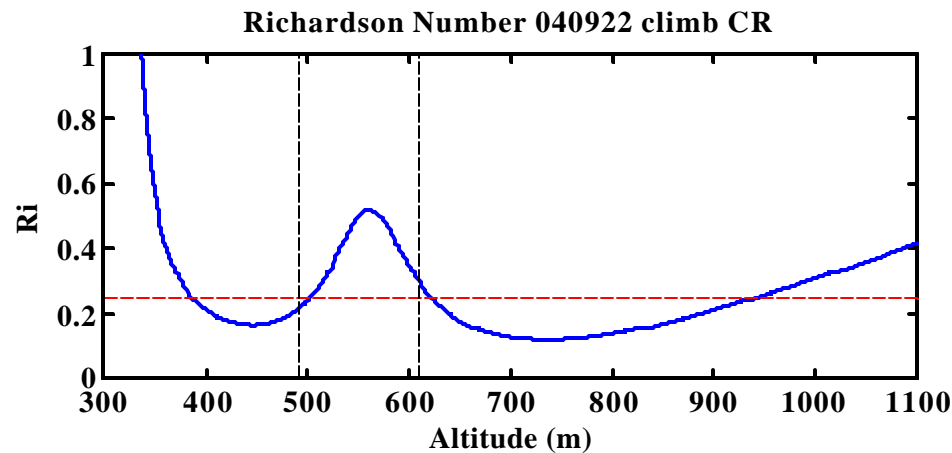
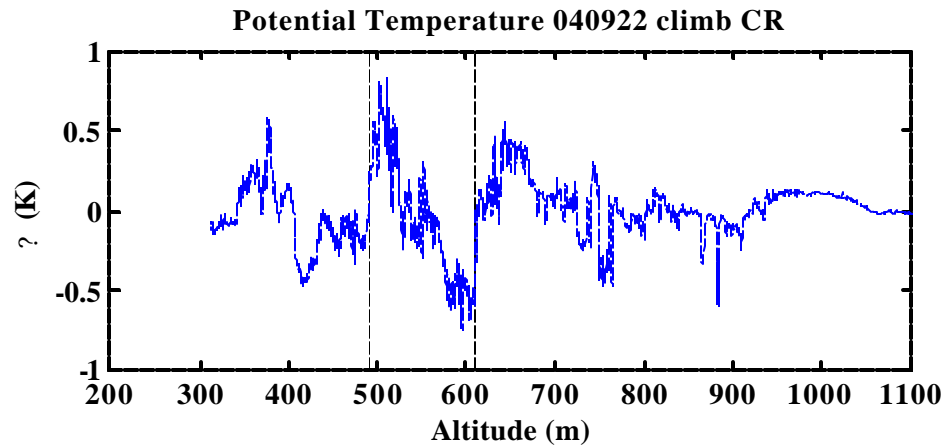


CLIMB PROFILES



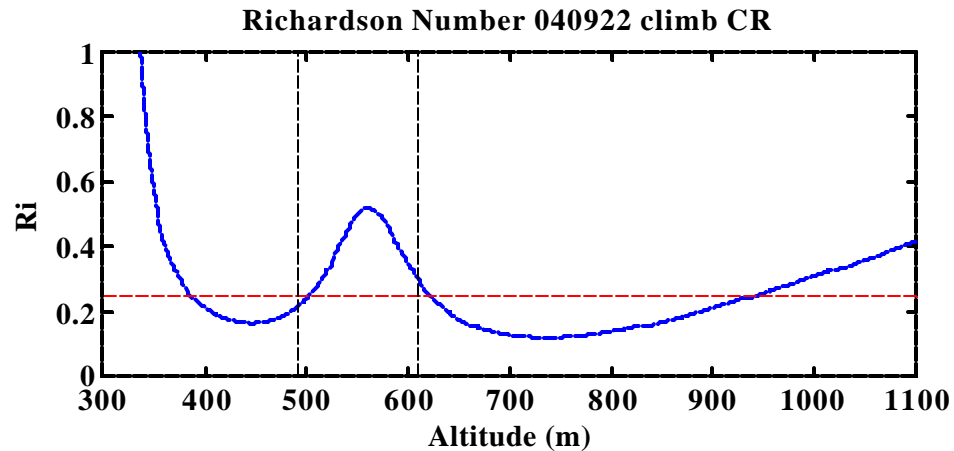
- Low pass filtered data (dashed lines)
 - 4th order Butterworth filter, with 0.01 Hz cutoff frequency (approx. 4.1 km horizontal distance or 350 m vertical distance)
 - Use to de-trend signals to better see CR behavior
 - Calculate vertical gradients.
- Zonal velocity is increasing (+ shear) but meridional velocity is decreasing (- shear)
- How does this affect CR versus RC?

HIGH PASS FILTERED POTENTIAL TEMPERATURE

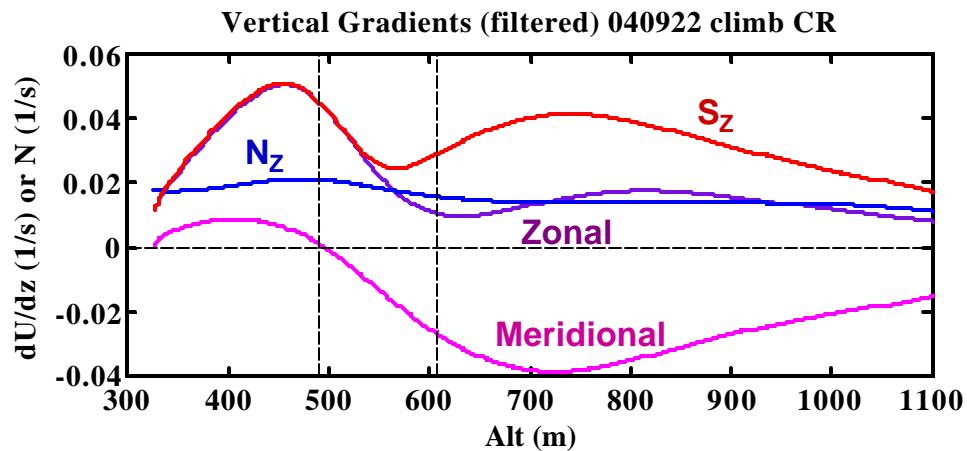


- High pass filtered using same cutoff frequency as low pass filtering (slide 2)
- CR structures clearly evident in detrended signal between 500 and 780 meter altitudes
 - 2 distinct cliffs.
 - Moderate turbulence
 - 250 meters high?
- Use gradients from low pass filter data to calculate Ri nos.
 - Ri well above 0.25 during waves
 - Ri decreases below 0.25 just before 1st cliff and after 2nd cliff

LOW PASS FILTERED GRADIENTS AND RI NOS.

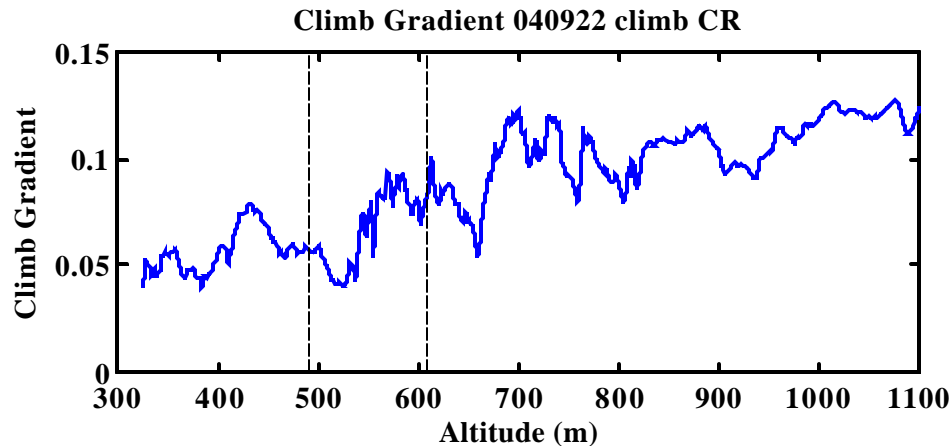
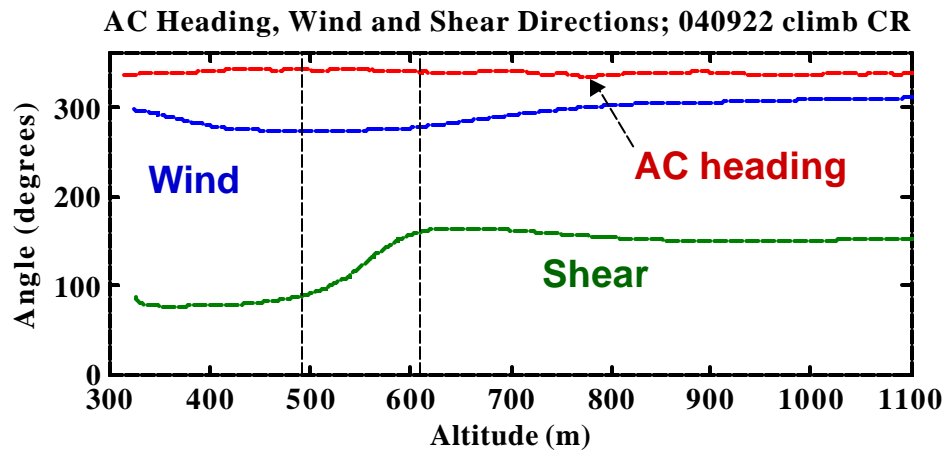


- Richardson number shows “hump” between first and second cliff
- Increasing Ri after first cliff is due to decreasing shear (S_z) relative Buoyancy frequency (N_z) due mainly to decreasing Zonal shear.



- Decreasing Ri before second cliff due to increasing (magnitude) of meridional shear.

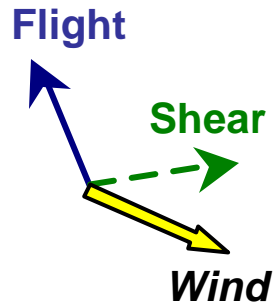
LOW PASS FILTERED DIRECTIONS



- Significant changes from first cliff to end of second ramp (around 750 m).
 - Wind direction changes 22°
 - Shear direction changes 71°.
 - This is due to increasing magnitude of meridional velocity and shear (see slides 2 and 4)
- Direction of wind and AC heading differ by an average of 62 degrees.
- Climb gradient increases from 0.05 (20:1) to 0.10 (10:1) during first CR

ORIENTATIONS

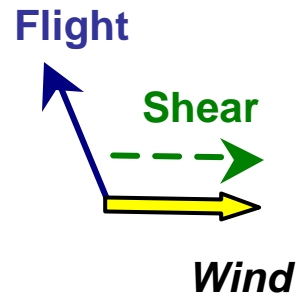
Before CRs



$$Dg_{SAC_WIND} = 43^\circ$$

$$Dg_{SAC_SHEAR} = 77^\circ$$

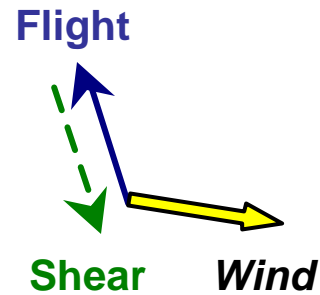
Cliff 1



$$Dg_{SAC_WIND} = 66^\circ$$

$$Dg_{SAC_SHEAR} = 67^\circ$$

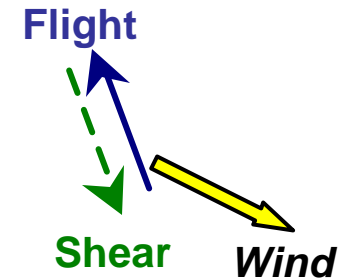
Cliff 2



$$Dg_{SAC_WIND} = 62^\circ$$

$$Dg_{SAC_SHEAR} = 1^\circ$$

After CRs

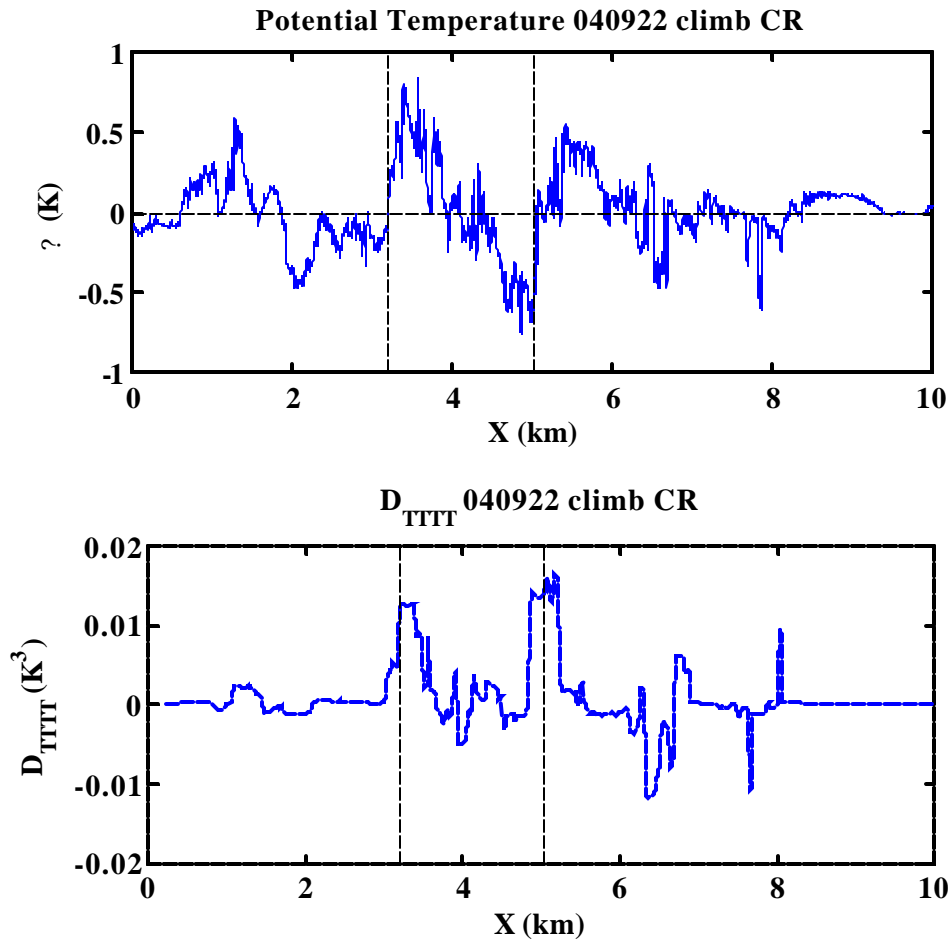


$$Dg_{SAC_WIND} = 43^\circ$$

$$Dg_{SAC_SHEAR} = 2^\circ$$

- This shows significant changes in shear direction during CRs
- Difference between wind and shear direction is about the same before and after CRs (43 degrees) and is about the same for the two cliffs (62-66 degrees)
- How are cliffs oriented? Only one probe, so can't determine from data

HIGH PASS FILTERED POTENTIAL TEMPERATURE



- Detrended data is plotted versus horizontal distance traveled.

- Wavelength in flight direction

- CR 1: 1.82 km

- CR 2: 1.34 km

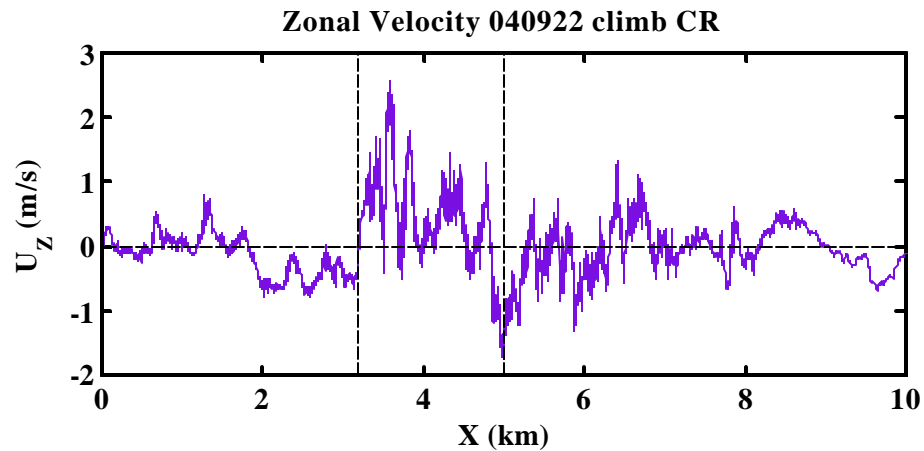
- If CRs are oriented in wind direction, then wavelengths are

- CR 1: 740 m

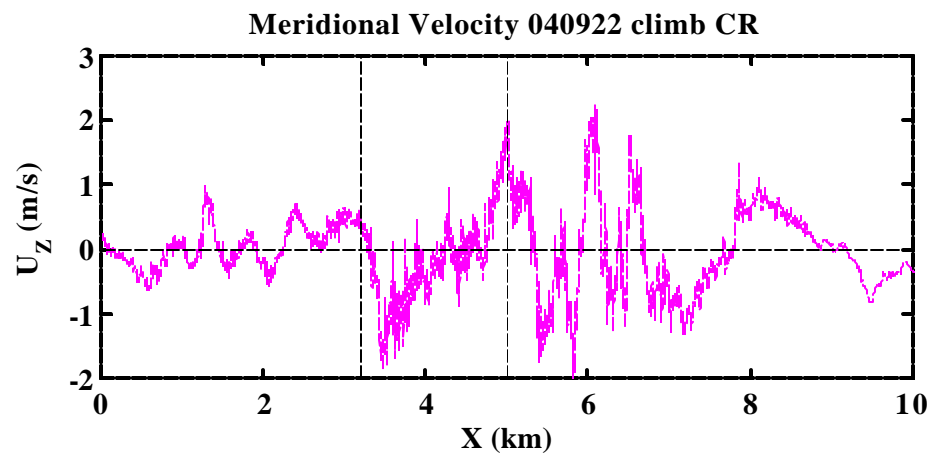
- CR 2: 630 m

- Third order structure function confirms cliffs.

HIGH PASS FILTERED POTENTIAL TEMPERATURE

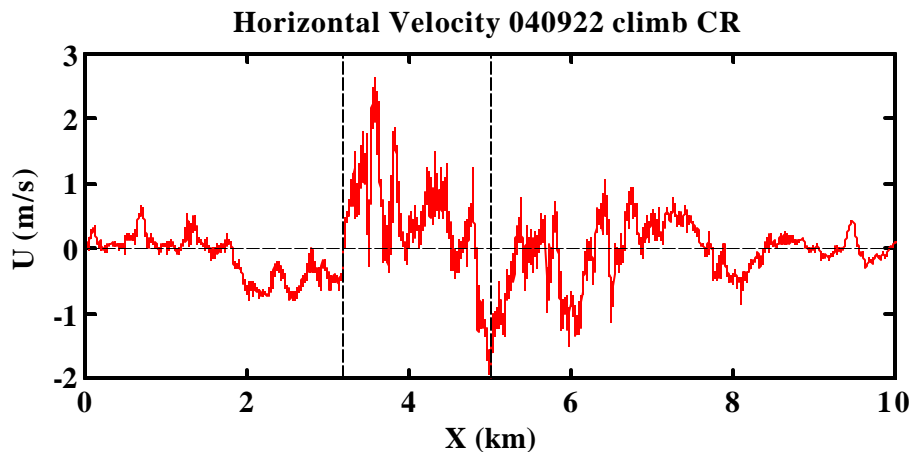
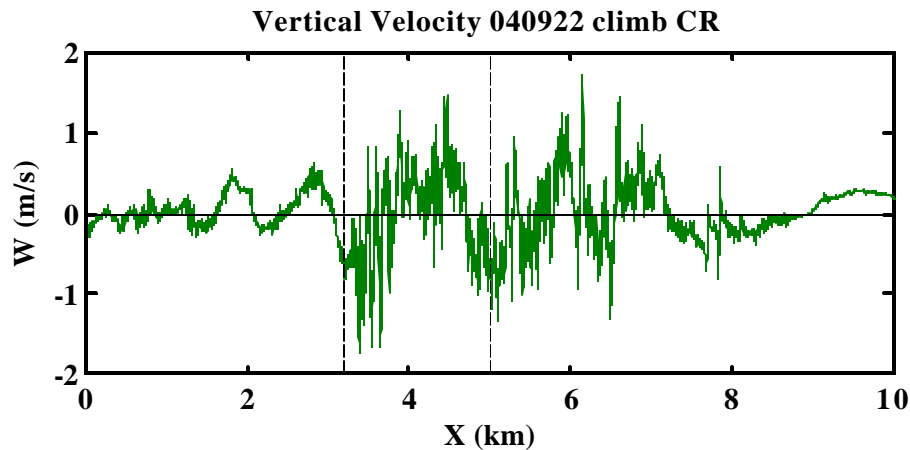


- Zonal velocity increase coincident with temperature cliffs



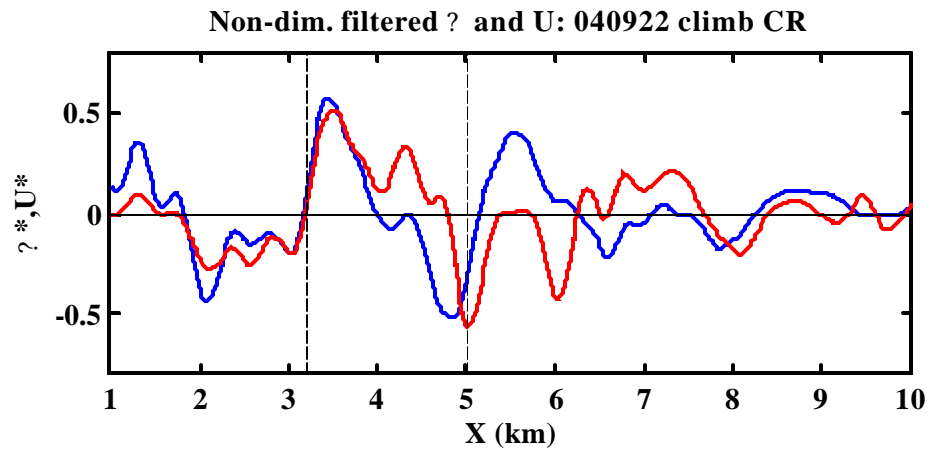
- Meridional velocity decrease coincident with temperature cliffs
- Consistent with negative vertical shear

HIGH PASS FILTERED POTENTIAL TEMPERATURE



- Vertical velocity fluctuations increase near cliffs
- Also show large scale pattern, though correlation with temperature unclear.
- Possible wave just before cliff?
- Horizontal velocity is velocity in mean wind direction (direction found from low pass filtered data).
- Essentially the same as zonal velocity for first CR, but includes contribution from meridional velocity during 2nd CR.

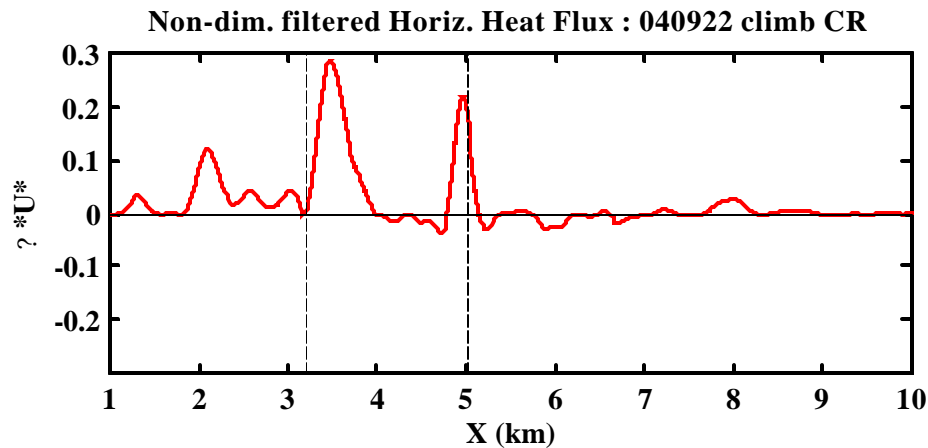
BAND-PASS FILTERED TEMP. AND HORIZ. VELOCITY



- Seems well correlated, though correlation coefficient is not as high as CR from other flights

$$C_{\theta^*U^*} = 0.48$$

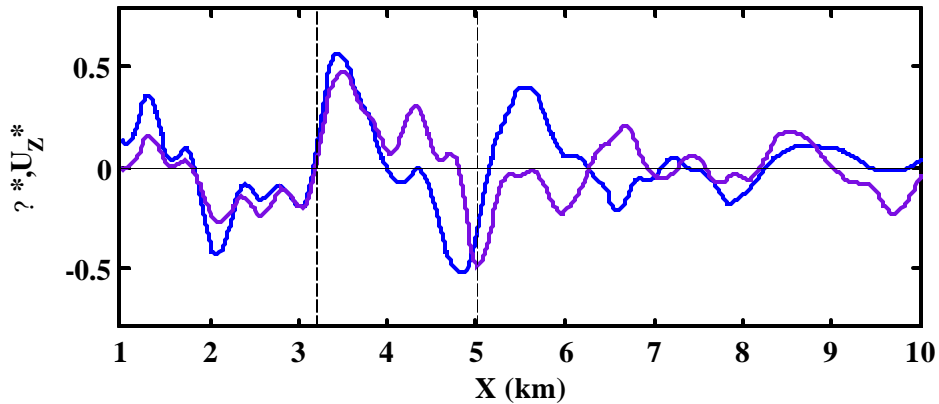
- Lower correlation coeff. could be due to phase shift around 2nd cliff.



- Heat flux dominated by cliff

BAND-PASS FILTERED TEMP. AND ZONAL VELOCITY

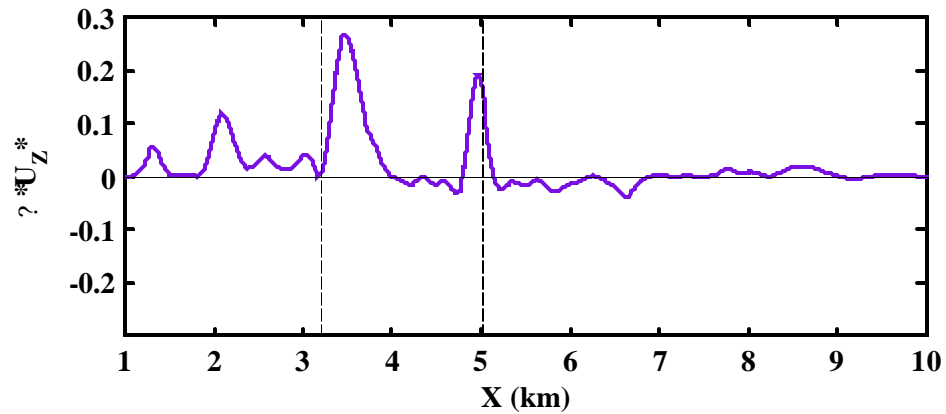
Non-dim. filtered θ and U_z : 040922 climb CR



- Behavior nearly the same as horizontal velocity (previous slide).

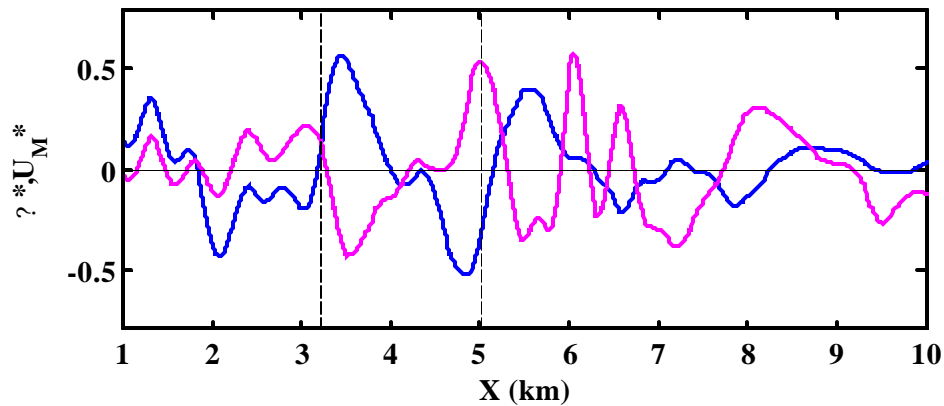
$$C_{Q*U_z^*} = 0.50$$

Non-dim. filtered Horiz. Heat Flux : 040922 climb CR



BAND-PASS FILTERED TEMP. AND MERID. VELOCITY

Non-dim. filtered? and U_M : 040922 climb CR

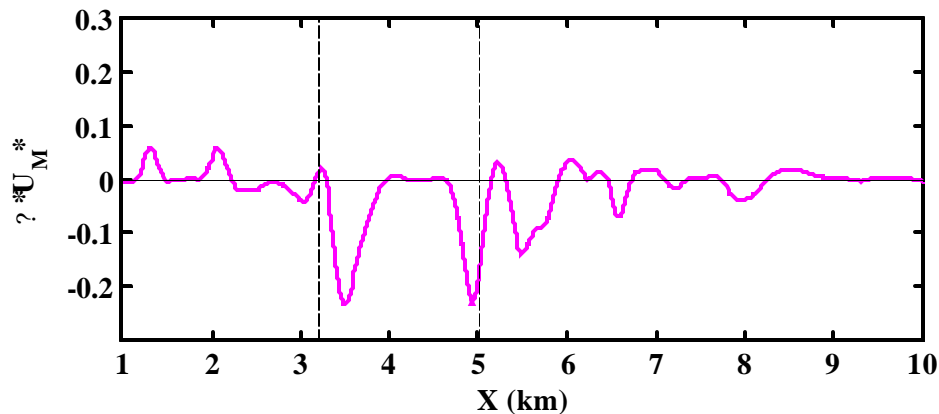


- Higher correlation coefficient than zonal or horiz.

$$C_{Q*U_M*} = -0.66$$

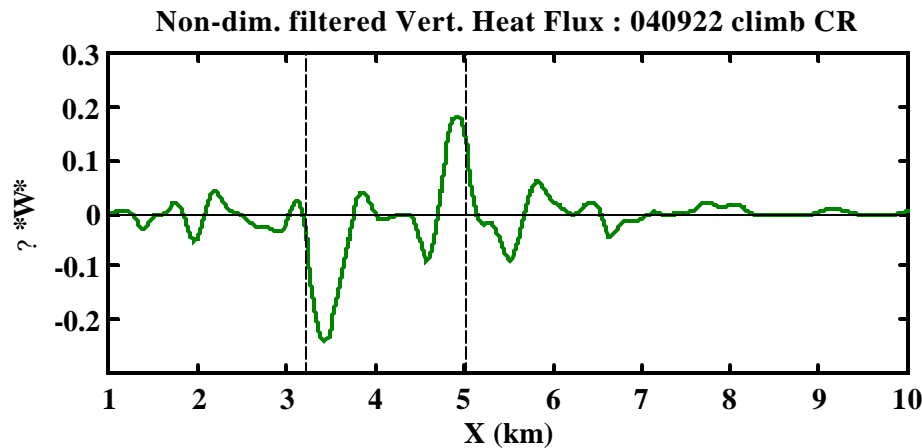
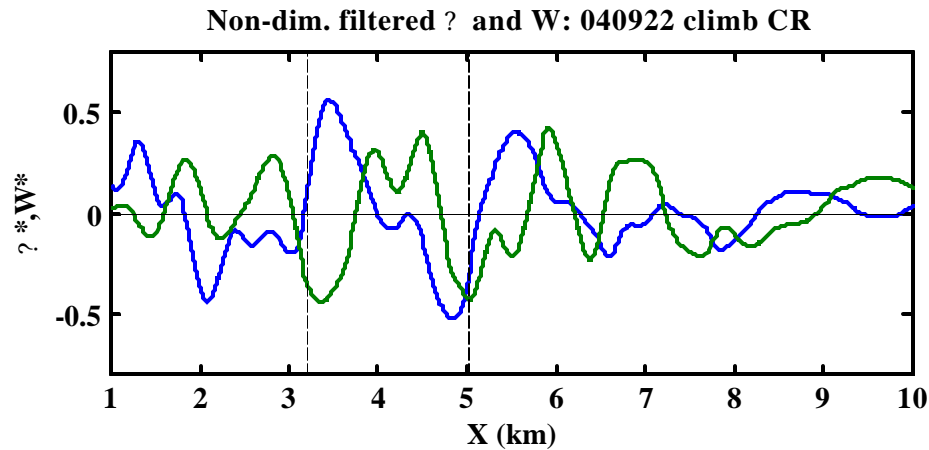
- Negative value consistent with negative vertical shear of U_M

Non-dim. filtered Horiz. Heat Flux : 040922 climb CR



- Heat flux negative and dominated by cliff response

BAND-PASS FILTERED TEMP. AND VERTICAL VELOCITY



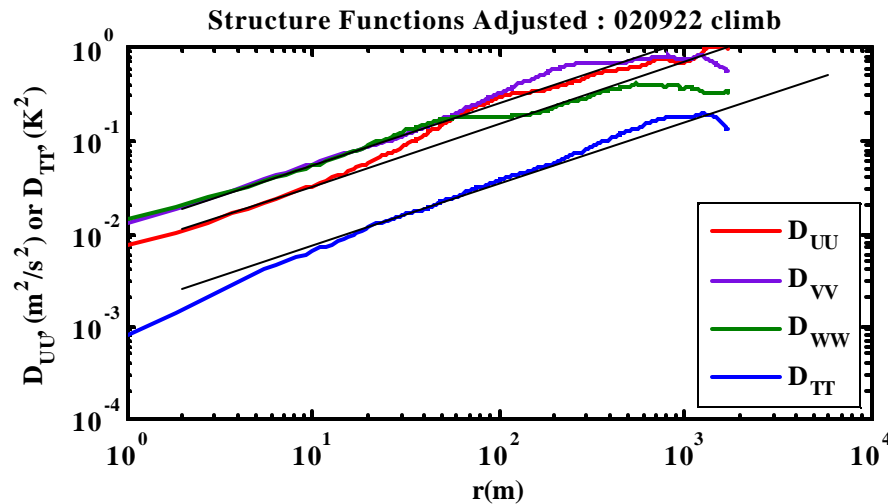
- Correlation between W and q is stronger than CR's from other flights, but its not consistent for the two cliffs

- Negative correlation for first cliff, and positive correlation for second cliff.

- Correlation coefficient about 30% lower than for CRs seen in other flights

$$C_{q^*W^*} = - 0.19$$

STRUCTURE FUNCTIONS & CONSTANTS



- Based on high pass filtered data
- solid black lines indicate 2/3 slope
- Structure constants for W and V are equal and much larger than those for U.

$$C_T^2 = 0.0016$$

$$C_U^2 = 0.0070 = 4.4 C_T^2$$

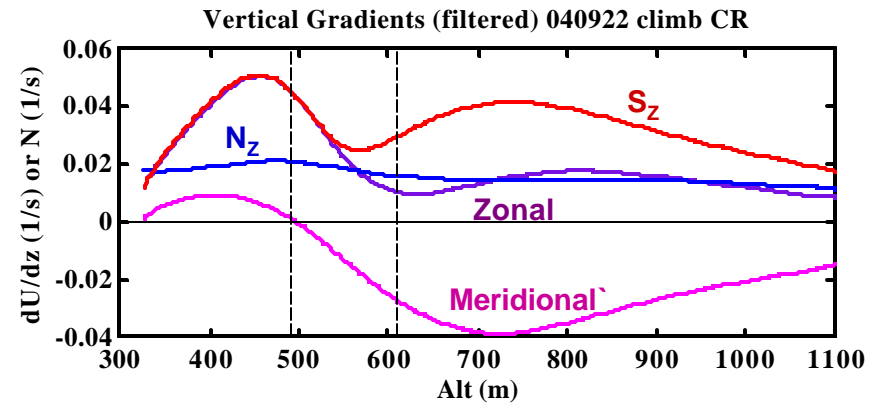
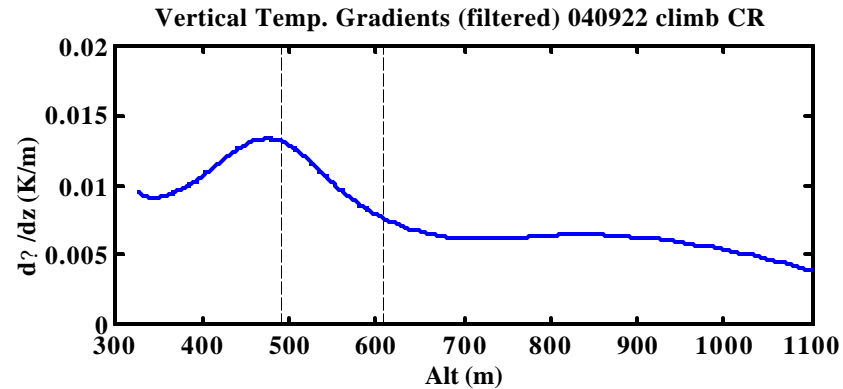
$$C_V^2 = C_W^2 = 0.0116 = 1.66 C_U^2$$

BILLOW HEIGHT ESTIMATE: GRADIENT ESTIMATE

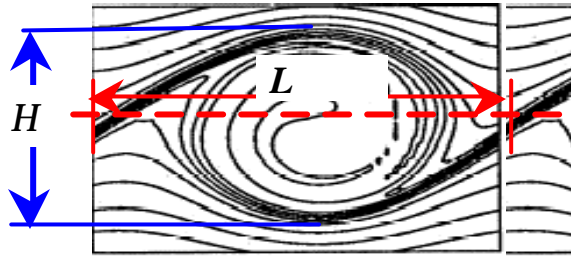
- Unlike CRs from other flights, vertical gradients are available as the AC climbs through the CR, but vertical gradients could be contaminated by horizontal changes, even though filtering was used.
- To be consistent with other cases, use gradients (both q and U) after CRs—shaded regions in plots.
- Gradients level off in this region.

$$\frac{dq}{dz} \gg 0.0062 \text{ K/m}$$

$$S_z \gg 0.0041/\text{s}$$



BILLOW HEIGHT AND ASPECT RATIO



	σ_q/σ_z (K/m)	Dq_{CLIFF} (K)	H (m)	L (m)	Aspect Ratio
Based on L in wind direction					
CR 1	0.0062	1.1	177	740	0.24
CR 2	0.0062	1.1	177	630	0.28

- Compare height of 177 meters with climb data that show vertical extent of CRs is about 250 m
 - 30% difference is consistent with comparisons with other estimates of height for CRs for other flights (e.g., see Briefing 1 page 29)
- Aspect ratios are similar to those found for CRs for other flights.

COMPARISON TO DNS AND OTHER CR'S: 040922 & 031122

- See Briefing 2 for details

Sykes, R. I. and W. S. Lewellen, A Numerical Study of Breaking Kelvin-Helmholtz Billows Using a Reynolds-Stress Turbulence Closure Model, *J. Atmos. Sci.*, 39, 1506-1520. (SL)

Scinocca, J. F., 1995, The mixing of Mass and Momentum by Kelvin-Helmholtz Billows, *J. Atmospheric Sciences*, 52, 2509-2530. (SC)

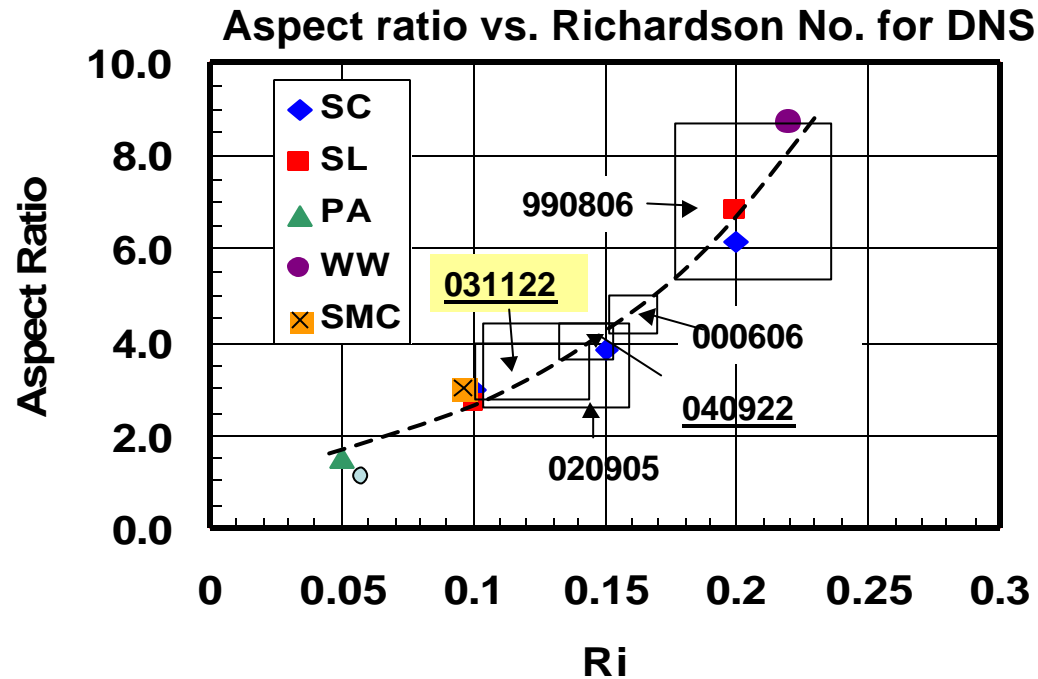
Palmer, TL, DC Fritts, Ø Andreassen and I Lie, 1994, Three-dimensional evolution of Kelvin Helmholtz billows in stratified turbulence, *Geophys. Res. Letters*, 21, 2287-2290 (PA)

Werne, J and DC Fritts, 1999, Stratified shear turbulence: evolution and statistics, *Geophys. Res. Letters*, 26, 439-442. (WF)

Smyth, WD and JM Moun, 2000, Length scales of turbulence in stably stratified mixing layers, *Phys. Fluids*, 12, 1327-1342 (SM)

Smyth, WD, JM Moun and DR Caldwell, 2001, The efficiency of mixing in turbulent patches: inferences from direct simulations and microstructure observations, *J. Phys. Oceanogr.*, 31, 1969-1992. (SMC)

COMPARISON TO DNS: ASPECT RATIO



- Use DNS to estimate range of initial Ri for CR using range of aspect ratios
 - Results for both 031122 and 040922 are very similar to those from 020905
 - Comparison with DNS suggests initial Ri of layer:
 - Between 0.1 and 0.14 for 031122 among the lowest of all 5 CR cases.
 - Between 0.13 and 0.15 for 040922
 - High aspect ratio of 990806 seems out of place compared to others

TURBULENCE SCALING: COMPARED TO OTHER CRS

Case	000606	020905	990806	040922	031122
S_z (1/s)	0.0318	0.0316	0.0220	0.00409	0.0123
H (m)	304	515	1,145	177	191
U_S (m/s) = $S_z H$	9.7	16.3	25.2	7.2	2.7
Dq_{CLIFF} (K)	2.1	4.4	4.6	1.1	0.43
$S_{U,FILT}$ (m/s)	0.407	0.766	1.66	0.210	0.1143
S_W (m/s)	0.514	0.807	1.76	0.376	0.1847
$S_{q,FILT}$ (K)	0.175	0.408	0.609	0.358	0.0386
$S_{U,FILT}/U_S$	0.042 (1)	0.047 (4)	0.066 (5)	0.043 (3)	0.042 (1)
S_W/U_S	0.053 (2)	0.050 (1)	0.070 (5)	0.065 (3)	0.069 (4)
$S_{q,FILT}/Dq_{CLIFF}$	0.082 (1)	0.093 (3)	0.133 (5)	0.103 (4)	0.089 (2)

- Expect higher scaled rms values for “older”, more turbulent layers.
 - Numbers in parenthesis show rank from “youngest” (1) to “oldest” (5)
- Trend in all scaled rms values is same for 000606, 020905 and 990806. (000606 and 020905 are similar, while 990806 is more turbulent).
- No consistent trend for 040922 or 031122

TURBULENCE SCALING: TRANSPORT

Turbulent diffusivity

$$n_{T,H} = \frac{- \langle w' q' \rangle}{\int Q / \int z}$$

Turbulent viscosity

$$n_{T,M} = \frac{- \langle u' w' \rangle}{\int u / \int z}$$

	$n_{T,H}$ m ² /s	$n_{T,M}$ m ² /s	$n_{T,M} / n_{T,H}$	$n_{T,H} / (HS_w)$	$n_{T,M} / (HS_w)$
000606	8.43	5.35	0.63	0.054	0.034
020905	26.9	12.6	0.47	0.065	0.030
990806	126	60.2	0.48	0.063	0.030
040922	3.45	1.49	0.46	0.041	0.019
031122	1.18	0.30	0.25	0.033	0.008

- Value for eddy diffusivity of heat for 040922 is close to those for the other 3 CR cases, but the value for 031122 is about 30-45% lower than the others.
- Values for eddy viscosity for 040922 are higher than the other cases (about 25%) and much lower for 031122 (50-60%)
- Generally, the comparisons for 040922 are promising, but the 031122 seem problematic.

COMPARISON TO **SMC** DNS: LENGTH SCALE ANALYSIS

$$L_O \gg \sqrt{\frac{e}{N^3}}$$

$$e \gg (C_U^2 / 2)^{1.5}$$

$$L_E \gg \frac{S_q}{\sqrt[3]{Q}}$$

$$L_B \gg \frac{S_w}{N}$$

Case	000606	020905	990806	040922	031122
$e (m^2/s^3)$	0.0029	0.0096	0.0322	0.000317	0.000105
$L_E (m)$	91.4	164	285	43.7	46.6
$L_O (m)$	31.8	50.9	160.4	10.4	13.3
$L_B (m)$	36.1	52.2	163.6	32.9	22.0
L_O/L_E	0.35 (4)	0.31 (3)	0.56 (5)	0.24 (1)	0.29 (1)
L_E/H	0.30 (2)	0.32 (1)	0.25 (4)	0.25 (4)	0.24 (3)
L_O/H	0.11 (4)	0.099 (3)	0.14 (5)	0.059 (1)	0.069 (2)
L_B/H	0.12	0.10	0.14	0.19	0.11

- SM & SMC DNS show that L_E decreases with time while L_O and L_O/L_E increase with time
- Numbers in parenthesis show rank from “youngest” (1) to “oldest” (5)
- Results for L_O and L_O/L_E for 031122 and 040922 indicate that they are relatively young layer similar to the 000606 and 020905 layers
- Results for L_E for 031122 and 040922 indicate that they are relatively mature layers similar to 990806.
- NOTE: Added L_B (not shown in Briefing 2)- trend is different than those for L_O and L_E

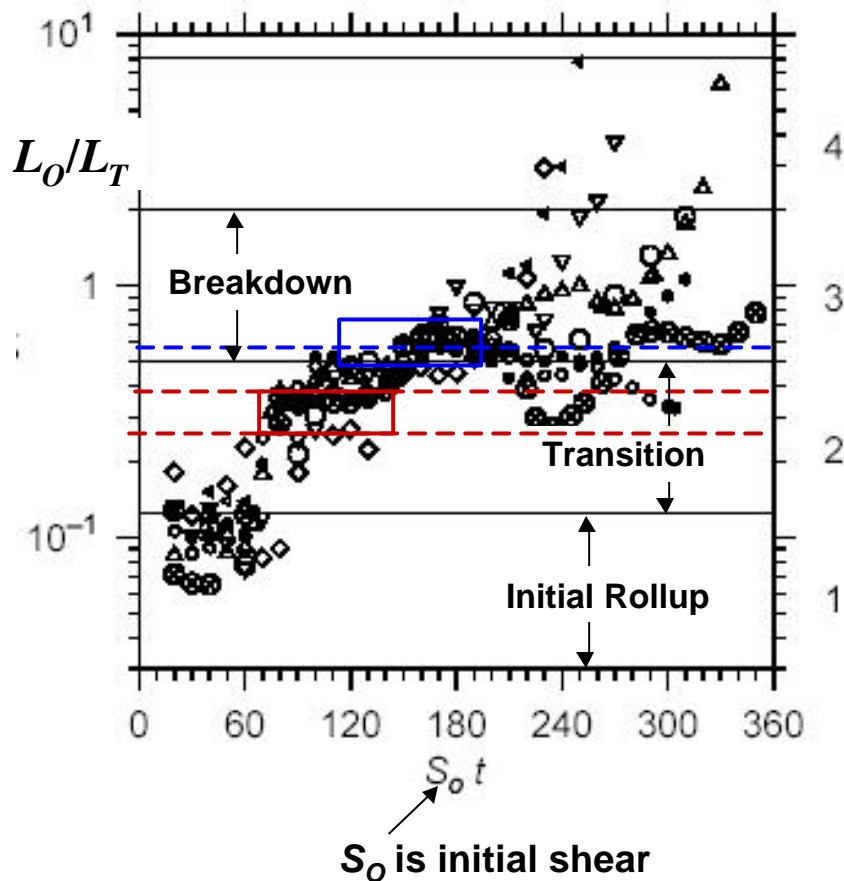
SUMMARY OF LAYER “AGE” ESTIMATE

	000606	020905	990806	040922	031122
Length Scale Comparison to DNS (Ranks: 1 is youngest, 5 is oldest)					
L_O/L_E	4	3	5	1	1
L_E/H	2	1	4	4	3
L_O/H	4	3	5	1	2
AVERAGE	3.3	2.3	4.7	2.0	2.0
Turbulence Scaling (Ranks: 1 is youngest, 5 is oldest)					
$s_{U, FILT}/U_S$	1	4	5	3	1
s_W/U_S	2	1	5	3	4
$s_{q, FILT}/Dq_{CLIFF}$	1	3	5	4	2
AVERAGE	1.3	2.7	5	3.3	2.3
OVERALL					
AVERAGE	2.5	2.5	4.83	2.7	2.2

- Overall, layer “age” estimates suggest that all layers are nearly the same “age” except for 990806, which seems to clearly be much older.

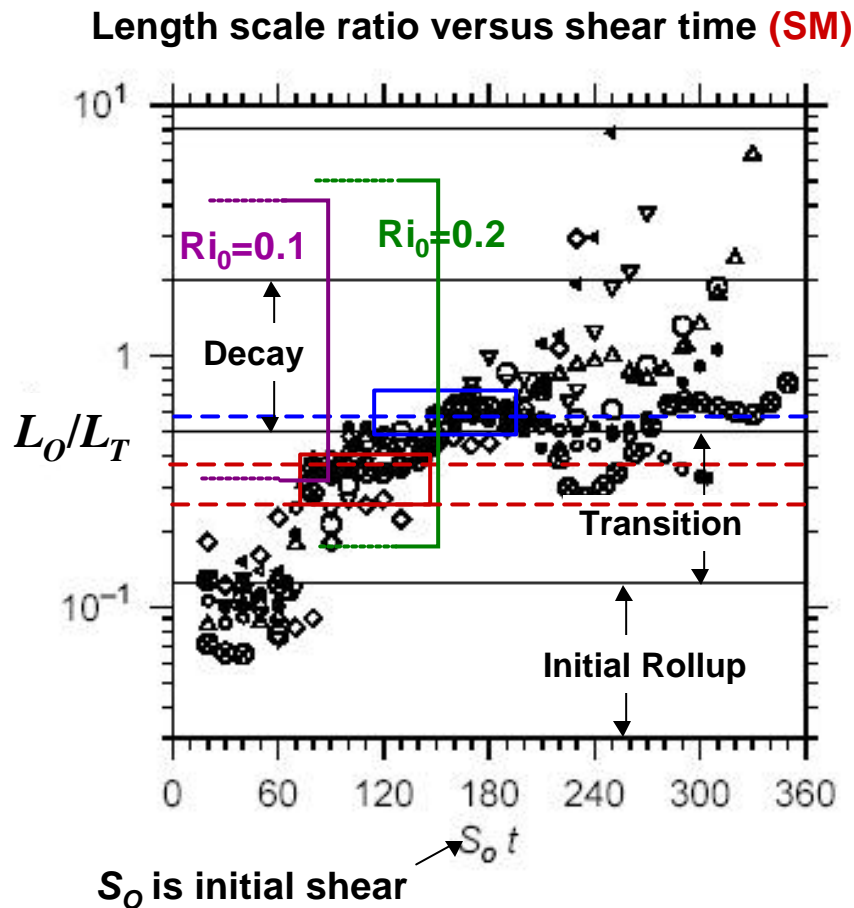
COMPARISON WITH **SM** & **SMC** DNS: TIME SCALE ANALYSIS

Length scale ratio versus shear time (**SM**)



- Note that the scatter suggests that using DNS to ‘finely’ distinguish layer age from data may be difficult.
- However, very promising that values of length scale ratio are similar to those from **SM**
- **000606, 020905, 040922, 031122** are consistent with transition (60 to 140 shear times)
- **990806** consistent with later stage transition and early breakdown (120 to 200 shear times)
- This is consistent with:
 - Idea that CR should be seen as long as braids are sharp (after roll-up)
 - Turbulence in signal, indicating that transition has occurred

PERSISTENCE OF CR PATTERN



- CR Should persist as long as there are distinct braids.
- Shaded rectangles show time over which sharp braids are seen in **SC** contour plots.
- Ranges from **SC** overlap time ranges from **SM** that correspond to calculated length scale ratios.
- This consistency between methods is strong evidence that KH are causing CR patterns.
- Also suggests initial Ri values consistent with those from aspect ratio analysis.
- **CR should persist at least 25 shear times:**
 - 000606 and 020905 – 13 min
 - 040922 – 14 min.
 - 990806 – 19 min.
 - 031122 – 30 min.

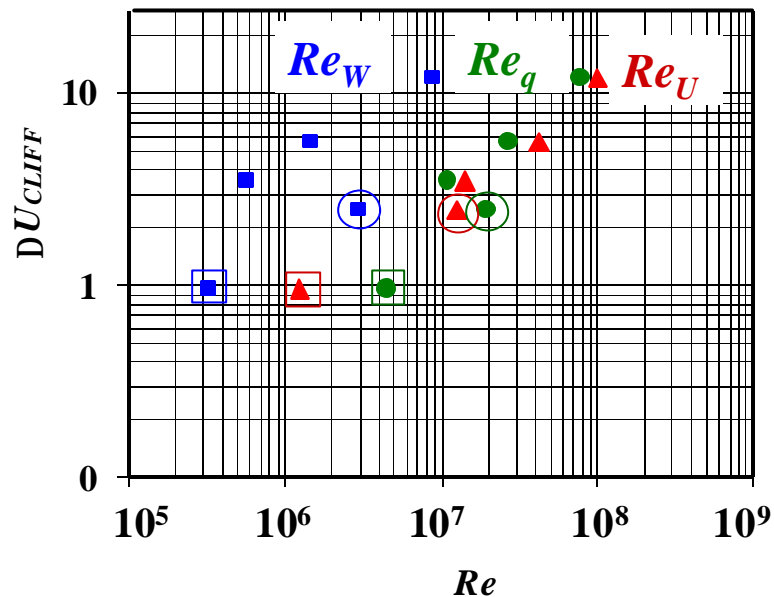
TURBULENT RE NUMBER-CLIFF VELOCITY CHANGE

Look at correlation between turbulent Reynolds numbers (3 different definitions) and change in velocity during cliff-ramps (DU_{CLIFF})

$$\text{Re}_w = \frac{S_w L_{DW}}{n} \quad L_{DW} = \frac{S_w^3}{e} \quad e = (C_U^2 / 2)^{3/2} \quad \text{Re}_U = \frac{S_U L_{DU}}{n}$$

$$q^2 = \frac{1}{2}(S_U^2 + S_V^2 + S_W^2)$$

- Data from 040922 case is circled, data from 031122 is marked with boxes.
- DU_{CLIFF} correlates well with Re except for 040922 case.



SUMMARY

- **031122 and 040922 are both weaker cliff-ramps than 000606, 020905 and 090806, but results confirmed earlier analysis of CRs from 000606, 020905 and 090806.**
- **Turbulence scaling and layer “age” analysis showed that all layers were similar (in terms of layer “age”, aspect ratio, and layer initial Ri) except for 090806.**
 - **090806 had higher aspect ratio (flatter billows), higher initial Ri and was an “older” layer. DNS results show that these are somewhat consistent—Higher initial Ri lead to flatter billows, which have turbulence transition within the ramps, rather than near the braids, and as such have distinct cliffs (braids) longer than lower Ri number.**
- **031122 exhibited some unique characteristics**
 - **May be a situation of a wave breaking, with the CR-KH layer forming at the peak temperatures during the wave.**
 - **Negative shear (measured during climbout) suggests RCs, like 000606—decreasing temperature during ramps – but temperature shows increase during ramps (CRs).**